

1 **Molecular corridors and parameterizations of volatility in the chemical
2 evolution of organic aerosols**

3

4

5 **Ying Li^{1,2}, Ulrich Pöschl¹, and Manabu Shiraiwa^{1,*}**

6

7 [1] Multiphase Chemistry Department, Max Planck Institute for Chemistry, Mainz, Germany

8 [2] State Key Laboratory of Atmospheric Boundary Layer Physics and Atmospheric Chemistry

9 (LAPC), Institute of Atmospheric Physics, Chinese Academy of Sciences, Beijing, China

10

11 *Correspondence to: M. Shiraiwa (m.shiraiwa@mpic.de)

12

13 *To be submitted to Atmospheric Chemistry and Physics (ACP)*

14

15

16 **Abstract:**

17 The formation and aging of organic aerosols (OA) proceed through multiple steps of chemical
18 reaction and mass transport in the gas and particle phases, which is challenging for the interpretation
19 of field measurements and laboratory experiments as well as accurate representation of OA
20 evolution in atmospheric aerosol models. Based on data from over 30,000 compounds, we show that
21 organic compounds with a wide variety of functional groups fall into molecular corridors,
22 characterized by a tight inverse correlation between molar mass and volatility. We developed
23 parameterizations to predict the saturation mass concentration of organic compounds containing
24 oxygen, nitrogen and sulfur from the elemental composition that can be measured by soft-ionization
25 high-resolution mass spectrometry. Field measurement data from new particle formation events,
26 biomass burning, cloud/fog processing, and indoor environments were mapped into molecular
27 corridors to characterize the chemical nature of the observed OA components. We found that less
28 oxidized indoor OA are constrained to a corridor of low molar mass and high volatility, whereas
29 highly oxygenated compounds in atmospheric water extend to high molar mass and low volatility.
30 Among the nitrogen- and sulfur-containing compounds identified in atmospheric aerosols, amines
31 tend to exhibit low molar mass and high volatility, whereas organonitrates and organosulfates
32 follow high O:C corridors extending to high molar mass and low volatility. We suggest that the
33 consideration of molar mass and molecular corridors can help to constrain volatility and particle
34 phase state in the modeling of OA particularly for nitrogen- and sulfur-containing compounds.

35

36 **1. Introduction**

37 Organic aerosols (OA) consist of a myriad of chemical species and account for a substantial
38 mass fraction (20–90 %) of the total submicron particles in the troposphere (Jimenez et al., 2009;
39 Nizkorodov et al., 2011). They influence regional and global climate by affecting radiative budget
40 of the atmosphere and serving as nuclei for cloud droplets and ice crystals (Kanakidou et al., 2005).
41 OA play a central role in air quality by causing haze formation in urban air (Huang et al., 2014;
42 Fuzzi et al., 2015; Zhang et al., 2015) and inducing adverse health effects (Pöschl and Shiraiwa,
43 2015). OA are introduced into the atmosphere either by being directly emitted from fossil fuel
44 combustion and biomass burning, or formed by multigenerational oxidation of gaseous precursors.
45 Secondary organic aerosols (SOA) pose a wide range of volatility, hygroscopicity and reactivity
46 (Hallquist et al., 2009). SOA evolution is a complex process involving both chemical reaction and
47 mass transport in the gas and particle phases (Kroll and Seinfeld, 2008; Ziemann and Atkinson,
48 2012; Shiraiwa et al., 2013a), but most aerosol models do not resolve multiphase processes
49 explicitly.

50 Several two-dimensional (2-D) frameworks have been proposed for efficient SOA
51 representation in chemical transport models. These 2-D frameworks were built based mainly on OA
52 properties including (effective) saturation mass concentration, number of carbon and oxygen atoms
53 in a molecule, mean carbon oxidation state, and atomic O:C or H:C ratios (Donahue et al., 2006;
54 Jimenez et al., 2009; Pankow and Barsanti, 2009; Heald et al., 2010; Donahue et al., 2011; Kroll et
55 al., 2011; Cappa and Wilson, 2012; Zhang and Seinfeld, 2013; Wania et al., 2014, 2015). Saturation
56 vapor pressure or the pure compound saturation mass concentration (C_0) is one of the key
57 thermodynamic properties describing the equilibrium gas-particle partitioning of organic
58 compounds (Pankow, 1994; Odum et al., 1996; Donahue et al., 2006; Krieger et al., 2012; Bilde et
59 al., 2015). Effective saturation mass concentration (C^*) or volatility includes the effect of non-ideal
60 thermodynamic mixing with an activity coefficient (γ): $C^* = \gamma C_0$ (Donahue et al., 2011, 2014; Zuend
61 and Seinfeld, 2012). The terms volatility and saturation mass concentration can be used

62 interchangeably with an ideal thermodynamic mixing assumption. The extent of importance of
63 non-ideal mixing depends strongly on contents of hydrophobic and hydrophilic organic compounds,
64 electrolytes and water (Zuend and Seinfeld, 2012; Shiraiwa et al., 2013b).

65 The volatility basis set (VBS) approach uses volatility and O:C ratio that can be constrained by
66 chamber experiments (Donahue et al., 2006, 2011, 2012). The total organic mass is classified into
67 volatility bins and their distribution between gas and aerosol phases is calculated according to
68 absorptive equilibrium partitioning assuming that gas-phase formation of semi-volatile organic
69 compounds as a limiting step of SOA formation (Pankow, 1994). VBS has been extensively applied
70 in chemical transport models, improving prediction of organic aerosol concentrations (Lane et al.,
71 2008; Tsimpidi et al., 2010; Shrivastava et al., 2011; Ahmadov et al., 2012; Jathar et al., 2012;
72 Murphy et al., 2012; Matsui et al., 2014; Morino et al., 2014; Tsimpidi et al., 2014).

73 Saturation mass concentration is a consequence of the molecular characteristics of molar mass,
74 chemical composition, and structure. Even though molar mass is an explicit parameter in computing
75 absorptive SOA partitioning (Pankow, 1994; Pankow and Barsanti, 2009), the current VBS method
76 does not account for the dependence of volatility on molar mass, assuming that the products
77 distributed in all volatility bins have the same value of molar mass, e.g., 150 g mol⁻¹ for
78 anthropogenic SOA and 180 g mol⁻¹ for biogenic SOA (Murphy and Pandis, 2009; Hayes et al.,
79 2015). Shiraiwa et al. (2014) have shown that SOA from a variety of biogenic and anthropogenic
80 precursors can be represented well by molecular corridors with a tight inverse correlation between
81 molar mass (M) and volatility of SOA oxidation products. The slope of these corridors corresponds
82 to the increase in molar mass required to decrease volatility by one order of magnitude. Molecular
83 corridors can help to constrain chemical and physical properties as well as reaction rates and
84 pathways with characteristic kinetic regimes of reaction-, diffusion-, or accommodation-limited
85 multiphase chemical kinetics involved in SOA evolution (Shiraiwa et al., 2014).

86 In recent years a high-resolution mass spectrometry (HR-MS) has been employed for
87 measurements on atmospheric aerosols, providing definitive determination of molar mass and

88 elemental composition (Tolocka et al., 2004; Reemtsma, 2009; Williams et al., 2010; Kampf et al.,
89 2011; Nizkorodov et al., 2011; Laskin et al., 2012; Chan et al., 2013; Hamilton et al., 2013;
90 Holzinger et al., 2013; Kourtchev et al., 2014). Soft ionization methods such as electrospray
91 ionization (ESI), atmospheric pressure chemical ionization (APCI), and direct analysis in real time
92 (DART) ionization are commonly applied for detailed molecular characterization, offering minimal
93 fragmentation of the analytes (Nozi ère et al., 2015 and references therein). Such measurements have
94 revealed that nitrogen- and sulfur- containing organic compounds are commonly present with a
95 substantial fraction of mass in atmospheric organic aerosols. A significant amount of N-heterocyclic
96 alkaloid and nitro-aromatic compounds were found in biomass burning plumes (Laskin et al., 2009;
97 Kitanovski et al., 2012). Organonitrates have been observed to account for a substantial fraction of
98 SOA in field and laboratory studies (Farmer et al., 2010; Rollins et al., 2012; Fry et al., 2013; Boyd
99 et al., 2015). Organosulfates have also been detected in ambient OA (Romero and Oehme, 2005;
100 Iinuma et al., 2007; Surratt et al., 2007, 2008; Luk ács et al., 2009; Ehn et al., 2010; Schmitt-Kopplin
101 et al., 2010; G ómez-Gonz ález et al., 2012; Lin et al., 2012; Stone et al., 2012; Kahnt et al., 2013;
102 Kundu et al., 2013; Ma et al., 2014; O'Brien et al., 2014; Staudt et al., 2014; Tao et al., 2014).
103 Reduced sulfur-containing compounds were observed in super-cooled clouds (Zhao et al., 2013) and
104 rainwater (Mead et al., 2015).

105 Although nitrogen- and sulfur- containing organic compounds are important components of
106 atmospheric aerosols, their physical properties and chemical behaviors are still poorly understood
107 (Nozi ère et al., 2015), and thus are untreated in air quality models so far. In this study, we apply the
108 molecular corridor-based approach to analyze ambient and indoor observations of organic aerosols
109 including nitrogen and sulfur containing organic compounds, to provide insights on the physical and
110 chemical processes driving OA evolution in the atmosphere.

111

112 **2. Characterization of 31066 organic compounds in molecular corridors**

113 More than thirty thousand organic compounds were analyzed to examine whether molecular
114 corridors can constrain a variety of organic compounds. The used dataset is the National Cancer
115 Institute (NCI) open database (<http://cactus.nci.nih.gov/download/nci/>), which contains 31,066
116 organic compounds and corresponding SMILES codes. A list of the compounds was also provided
117 in Wei et al. (2012). Saturation vapor pressure of each compound was estimated by the Estimation
118 Programs Interface (EPI) Suite software (version 4.1) developed by the U.S. Environmental
119 Protection Agency (US EPA, 2015). The EPI Suite reports vapor pressure calculated in three
120 separate methods, including the Antoine method (Lyman et al., 1990), the modified Grain method
121 (Lyman, 1985), and the Mackay method (Lyman, 1985). In this study, the modified Grain estimate
122 was used for solids and the average of the Antoine and the modified Grain estimates was used for
123 liquids and gases, following the suggestions of the EPI Suite. The vapor pressure was then
124 converted to the saturation mass concentration (C_0 in $\mu\text{g m}^{-3}$) through the relationship:

125
$$C_0 = \frac{M10^6 p_0}{760RT} \quad (1)$$

126 where M is the molar mass (g mol^{-1}), p_0 is the saturation vapor pressure (mm Hg), R is the ideal gas
127 constant ($8.205 \times 10^{-5} \text{ atm K}^{-1} \text{ mol}^{-1} \text{ m}^3$) and T is the temperature (K).

128 We classified these organic compounds into six classes based on chemical composition: CH,
129 CHO, CHN, CHON, CHOS, and CHONS, with the number of compounds of 328, 8420, 2968,
130 13628, 925, and 3367, respectively. These compounds cover a molar mass from 41 to 1779 g mol^{-1} .
131 In total we consider 22 structural sub-classes including N-containing compounds of amine (primary,
132 secondary, tertiary, and quaternary), amide, azo, azide, amino acid, imine, nitroso, nitro, alkyl nitrite,
133 nitrile and organonitrate as well as S-containing compounds of organosulfate, sulfonate, sulfone,
134 sulfoxide, sulfite, heterocyclic ring, thioate, and thiocarbamate.

135 Figure 1 shows that most of the organic compounds (small markers color-coded by atomic O:C
136 ratio) fall into the molecular corridor with upper and lower boundaries represented by linear alkanes
137 ($\text{C}_n\text{H}_{2n+2}$, O:C=0, purple dashed line) and sugar alcohols ($\text{C}_n\text{H}_{2n+2}\text{O}_n$, O:C=1, red dashed line),
138 respectively. It indicates that the 2-D space of molar mass and saturation mass concentration can

139 constrain most of the organics, including compounds containing heteroatoms of N and S. About
140 1000 compounds with branched structures lie above the linear alkane line among the CHO class
141 (Fig. 1b), as volatilities of branched compounds are higher than those of compounds with linear
142 structures. The surrogate compounds with the mean values of M , C_0 , and O:C ratio computed for
143 each of the structural sub-classes are indicated by larger symbols with error bars indicating standard
144 deviations. Fig. 1c shows clearly that mean values of C_0 decrease as more hydrogen atoms of an
145 ammonia structure are replaced by alkyl or aryl groups, forming the primary-, secondary-, tertiary-
146 and quaternary-amine. Figure 1d-f show that the molar mass of CHON, CHOS, and CHONS can be
147 up to 1000 g mol⁻¹ and C_0 can be as low as 10⁻³⁰ µg m⁻³. The compounds with high O:C ratios are
148 organosulfate and sulfite (the mean O:C of ~ 1), followed by compounds in sub-classes of sulfonate,
149 sulfone, sulfoxide, organonitrate, nitro, alkyl nitrites, nitroso, or amino acid, which tend to occupy
150 the space close to the sugar alcohol line.

151 OA can be classified as (1) volatile organic compounds (VOC, $C_0 > 3 \times 10^6$ µg m⁻³), (2)
152 intermediate volatility OC (IVOC, $300 < C_0 < 3 \times 10^6$ µg m⁻³), (3) semi-volatile OC (SVOC, $0.3 < C_0$
153 < 300 µg m⁻³), (4) low-volatile OC (LVOC, $3 \times 10^{-4} < C_0 < 0.3$ µg m⁻³), and (5) extremely
154 low-volatile OC (ELVOC, $C_0 < 3 \times 10^{-4}$ µg m⁻³) (Donahue et al., 2011; Murphy et al., 2014). Figure
155 2 shows the relationship between saturation mass concentration and molar mass derived from these
156 thirty thousand compounds. The molar mass of VOC is usually less than 160 g mol⁻¹; 130 – 250 g
157 mol⁻¹ for IVOC, 180 – 330 g mol⁻¹ for SVOC, 210 – 400 g mol⁻¹ for LVOC, and larger than 260 g
158 mol⁻¹ for ELVOC. As the volatility decreases, the covered molar mass range becomes wider,
159 indicating more compounds are encompassed with increasing complexity. Meanwhile, the volatility
160 decreases as the average molar mass of every composition group increases. For example, the
161 average molar mass of the CHO class in the VOC group is 117 g mol⁻¹, which increases to 471 g
162 mol⁻¹ in the ELVOC group. The symbol sizes are scaled with relative abundance of compounds in
163 each composition class. Many of the CH compounds (~69%) are distributed in the VOC and IVOC
164 groups. 70% of the CHO and CHN compounds are populated in the IVOC and SVOC groups. More

165 than 80% of the CHON and CHOS compounds are located in the range covering from IVOC to
166 LVOC, and about 10% of them belong to the ELVOC group. 90% of the CHONS compounds cover
167 the range from SVOC to ELVOC. Given that the molar mass is observationally constrained, it is
168 suitable to use the molar mass to constrain the volatility of organic compounds.

169

170 **3 Parameterization of saturation mass concentration by elemental composition**

171 Accurate prediction of volatility requires structural information of the organic compounds,
172 which is often difficult to be obtained in field measurements. We predict C_0 as a function of
173 elemental composition that is often determined by soft-ionization high-resolution mass spectrometry.
174 Donahue et al. (2011) has developed a parameterization to estimate C_0 as $\log_{10}C_0 = f(n_C, n_O)$ for
175 the CHO compounds. We broaden this formulation to $\log_{10}C_0 = f(n_C, n_O, n_N, n_S)$ to be applicable
176 to the N and S-containing compounds:

$$177 \log_{10}C_0 = (n_C^0 - n_C)b_C - n_O b_O - 2 \frac{n_C n_O}{n_C + n_O} b_{CO} - n_N b_N - n_S b_S \quad (2)$$

178 where n_C^0 is the reference carbon number; n_C , n_O , n_N , and n_S denote the numbers of carbon,
179 oxygen, nitrogen, and sulfur atoms, respectively; b_C , b_O , b_N , and b_S denote the contribution of
180 each atom to $\log_{10}C_0$, respectively, and b_{CO} is the carbon-oxygen nonideality (Donahue et al.,
181 2011). Values of b coefficients were obtained by fitting with multi-linear least squares analysis to
182 the thirty thousand compounds for each class (CH, CHO, CHN, CHON, CHOS, and CHONS). The
183 best-fit parameters obtained at 298 K in this analysis are presented in Table 1. The non-linear terms
184 of nitrogen-oxygen and sulfur-oxygen are not considered, as they impact the predicting results only
185 slightly. Considering the number of hydrogen atoms in Eq. (2) could improve the prediction for
186 compounds in the CH class slightly, but have little impact on the prediction for compounds in other
187 composition classes. Detailed information including an estimated b_H (the contribution of hydrogen
188 atoms to $\log_{10}C_0$) can be found in the Supplement. As the effect of inclusion of hydrogen is limited,
189 further analysis was conducted using Eq. (2) for simplicity.

190 The temperature dependence of C_0 can be approximated by an Arrhenius type equation
191 resembling the Clausius Clapeyron equation (Donahue et al., 2006; Cappa and Jimenez, 2010):

192
$$C_0(T) = C_0(T_{\text{ref}}) \left(\frac{T_{\text{ref}}}{T} \right) \exp \left[-\frac{\Delta H_{\text{vap}}}{R} \left(\frac{1}{T} - \frac{1}{T_{\text{ref}}} \right) \right] \quad (3)$$

193 where T_{ref} is the temperature at a reference state (298 K in this study). The enthalpy of vaporization
194 ΔH_{vap} (kJ mol⁻¹) could be estimated by C_0 , as there is a nearly linear relationship between $\log_{10}C_0$
195 (300K) and ΔH_{vap} (Epstein et al., 2010).

196 The developed estimation method was compared with the EPI Suite for the thirty thousand
197 compounds as shown in Fig. 3 and Table S2. The agreement between the two methods was assessed
198 by statistical measures of correlation coefficient (R), mean absolute gross error (MAGE), and mean
199 bias (MB). As shown in Fig. 3, our new method performs well with R above 0.8 and MAGE below
200 1.8 for all the composition classes. In the CHN class, our method performs well for primary,
201 secondary, and tertiary amines, heterocyclic rings, imines and nitriles (Table S2). Our method
202 overestimates C_0 of the quaternary amine located in LVOC and ELVOC ranges. For the CHON
203 class, relatively large errors are found for quaternary amine and amino acid. Note that there are
204 relatively few data for organonitrate. When nitrate functionality appears in the amine, they are
205 assigned to the amine class. Nitroso and alkyl nitrite are treated similarly. For structural classes in
206 the CHOS and CHONS, our method works well with $R > 0.82$.

207 Our method was also tested with a different set of organic compounds and a different
208 estimation method. We used 704 SOA oxidation products of CHO compounds (Shiraiwa et al., 2014)
209 with saturation vapor pressure estimated using the EVAPORATION model (Compernolle et al.,
210 2011). As shown in Fig. 4(a), our newly developed parameterization also agrees well with
211 EVAPORATION predictions, showing better agreement than Donahue et al. (2011), as indicated by
212 smaller values of MB and MAGE. Figure 4(b) shows the comparison between C_0 estimated by our
213 parameterization and the experimental data. The experimental C_0 values of 1729 organic
214 compounds with heteroatoms including N or S are taken from the PHYSPROP database that is part

215 of the EPI Suite (<http://esc.syrres.com/interkow/EpiSuiteData.htm>). Our method gives a good
216 performance with R of 0.84, MB of -0.41, and MAGE of 1.24.

217 As shown in Fig. 4(b), the estimation error increases as the saturation mass concentration
218 decreases. An accurate prediction of low vapor pressure is difficult due, in large part, to the
219 limitation caused by measurement challenges. For example, the measured vapor pressure of
220 dicarboxylic acid, a low-volatility compound commonly found in atmospheric aerosols, disagreed
221 by up to two orders of magnitude between different measurement techniques (Krieger et al., 2012;
222 Huisman et al., 2013; Bilde et al., 2015). The effects of functionalization, phase states (crystalline,
223 amorphous, (subcooled) liquid), and molecular structure need to be considered in future
224 experimental studies (Huisman et al., 2013; Bilde et al., 2015). The vapor pressure estimation
225 methods could give very divergent predictions for the same compound (Clegg et al., 2008; O'Meara
226 et al., 2014). Another difficulty in predicting low vapor pressure is that most estimation methods,
227 including the EPI Suite, are constrained by databases heavily biased toward mono-functional
228 compounds with saturation vapor pressures in the range of $\sim 10^3$ – 10^5 Pa (Barley and McFiggans,
229 2010; Krieger et al., 2012). The EPI Suite uses the PHYSPROP database as its training data set.
230 When comparing with the PHYSPROP database, the estimation error of EPI Suite increases as the
231 vapor pressure decreases, especially when the vapor pressure decreases below 10^4 Pa
232 (<http://www.epa.gov/sab/pdf/sab-07-011.pdf>).

233 Despite of some limitations as described above, the new estimation parameterization derived
234 from a large dataset in this study is sufficiently good to predict C_0 for various structural organic
235 classes as shown by overall good correlation. In the next section, the saturation mass concentration
236 of ambient OA (e.g., the compounds with elemental composition measured by high-resolution mass
237 spectrometry techniques) is estimated using Eq .(2).

238
239 **4 Application of molecular corridors to atmospheric aerosols**

240 Applying the newly developed saturation mass concentration estimation method to laboratory
241 experiments and field campaigns, the observed organic compounds were mapped into the molecular
242 corridor with an alternative representation displaying C_0 as a function of molar mass, which appears
243 more straightforward for direct comparisons to mass spectra (Shiraiwa et al., 2014). The used
244 observation dataset is summarized in Table 2. In total 9053 organic compounds were collected from
245 chamber experiments for new particle formation (Ehn et al., 2012; Schobesberger et al., 2013) and
246 field measurements at a boreal forest (Ehn et al., 2010, 2012), at a mountain site (Holzinger et al.,
247 2010), in urban areas (Lin et al., 2012; Stone et al., 2012; Ma et al., 2014; O'Brien et al., 2014; Tao
248 et al., 2014), in biomass burning plumes (Laskin et al., 2009), in radiation fog (Mazzoleni et al.,
249 2010), in super-cooled cloud (Zhao et al., 2013), and in rain (Altieri et al., 2009a, 2009b, 2012) as
250 well as indoor measurements of OA originated from tobacco smoke (Sleiman et al., 2010a, 2010b)
251 and human skin lipids (Wisthaler and Weschler, 2010). The organic compounds were categorized
252 into CH (55), CHO (3042), CHN (152), CHON (4074), CHOS (954), and CHONS (776) classes.
253 These large data sets provide insights into the chemical and physical nature of OA from different
254 sources and their evolution upon chemical transformation.

255

256 **4.1 CH and CHO compounds**

257 Figure 5 shows the CH and CHO compounds measured in different atmospheric conditions
258 plotted in molecular corridors. The small markers show individual observed compounds
259 color-coded by atomic O:C ratio. The larger symbols with error bars represent mean values of molar
260 mass, saturation mass concentration, and O:C ratio derived from every observation event. Figure 5a
261 shows abundant organic compounds found in new particle formation (NPF) experiments performed
262 at the Cosmics Leaving Outdoor Droplets (CLOUD) chamber at CERN (Schobesberger et al., 2013)
263 and the Jülich Plant Atmosphere Chamber (Mentel et al., 2009; Ehn et al., 2012). The values of O:C
264 ratio are all above 0.3 and some organic compounds are remarkably highly oxidized (O:C up to 1.4).
265 The compounds cover the mass range of $184 - 558 \text{ g mol}^{-1}$ in the volatility range of IVOC –

266 ELVOC, spreading in a large space of the molecular corridor. These oxidized organic compounds
267 play an important role in formation and growth of OA particles in ambient conditions (Ehn et al.,
268 2012; Riipinen et al., 2012; Kulmala et al., 2013; Schobesberger et al., 2013; Ehn et al., 2014;
269 Riccobono et al., 2014; Wildt et al., 2014).

270 Figure 5b shows highly oxidized compounds observed at the boreal forest research station in
271 Hyytiälä, Finland during NPF events (Ehn et al., 2010, 2012). The average O:C ratio is as high as
272 1.1. The locations of organic compounds observed in the CLOUD experiments (Fig. 5a) and at
273 Hyytiälä (Fig. 5b) in the molecular corridor are similar by occupying the space close to the sugar
274 alcohol line (high O:C corridor; Shiraiwa et al., 2014), indicating that chemical properties of these
275 organic compounds are similar and chamber experiments represent ambient observations well. Such
276 low-volatility and highly oxygenated compounds may be generated by autoxidation reactions
277 (Crounse et al., 2013; Ehn et al., 2014; Mentel et al., 2015).

278 Figure 5c shows organic compounds observed in the remote area at the Mt. Sonnblick, Austria
279 (Holzinger et al., 2010). The observed compounds were less oxidized and lie close to the alkane line.
280 Aqueous-phase processing of organic compounds leads to formation of highly oxidized compounds
281 in fog (Fig. 5d; Mazzoleni et al., 2010), cloud (Fig. 5e; Zhao et al., 2013) and rain (Fig. 5f; Altieri et
282 al., 2009a, 2009b, 2012) suggesting that atmospheric water is enriched in polar compounds
283 compared to atmospheric particulate matter. Higher oxidized compounds tend to have lower molar
284 mass than less oxidized compounds, indicating that fragmentation is an important pathway in
285 aqueous-phase oxidation (Sun et al., 2010; McNeill et al., 2012; Carlton and Trupin, 2013; Daumit
286 et al., 2014; Erven 2015). In addition, aqueous processing can produce high molar-mass and high
287 O:C compounds through oligomerization (Altieri et al., 2008; Lim et al., 2010; Ervens et al.,
288 2011), as seen in super-cooled cloud water collected at a remote site on the Mt. Werner in the U.S.
289 in Fig. 5e.

290 Figure 5g shows the oxidation products from reactions of ozone and human skin lipids
291 (Wisthaler and Weschler, 2010). The majority of products are VOC and IVOC with O:C <0.7 and

292 molar mass <200 g mol⁻¹, mainly occupying the space close to the origin of the molecular corridor.
293 Some products with higher molar mass (>300 g mol⁻¹) are mainly first-generation products of
294 ozonolysis of skin lipids, including hydroxyl geranyl acetone, polyunsaturated aldehydes and fatty
295 acids. These products can be further oxidized by ozone, generating fragmented secondary products
296 with a relatively higher O:C ratio with carbonyl, carboxyl, or α -hydroxy ketone groups (Wisthaler
297 and Weschler, 2010).

298 Cigarette smoke is another pollutant frequently encountered in indoor air and residual
299 secondhand tobacco smoke absorbed to indoor surfaces can react with atmospheric species such as
300 ozone (Destaillets et al., 2006; Sleiman et al., 2010a) and nitrous acid (HONO) (Sleiman et al.,
301 2010b) to form thirdhand smoke hazards. As shown in Fig. 5h, most of the nicotine products have
302 $M < 300 \text{ g mol}^{-1}$ and O:C < 0.5 with $\log_{10}C_0 > 2 \mu\text{g m}^{-3}$. As oxidant levels in indoor air are relatively
303 low compared to outdoor air (Weschler, 2011), indoor OA tend to be less oxidized and have lower
304 molar mass.

305

306 **4.2 Nitrogen- and sulfur-containing compounds**

307 Figure 6 shows N-containing compounds plotted in the molecular corridor. Figure 6a shows 23
308 compounds observed at Hyytiälä, Finland during NPF events (Ehn et al., 2010, 2012). They are
309 mainly amines with a small molar mass range (69 – 169 g mol⁻¹) and intermediate volatility,
310 covering the space close to the origin of the molecular corridor. Amines can stabilize sulfuric acid
311 clusters efficiently and their role in nucleation may be significant (Loukonen et al., 2010; Smith et
312 al., 2010; Wang et al., 2010; Erupe et al., 2011; Zhang et al., 2011; Kulmala et al., 2014).

313 N-containing organic compounds are important components of biomass-burning organic
314 aerosols (BBOA) (Lobert et al., 1990; Simoneit, 2002). Figure 6b presents these compounds
315 including amine, urea, alkyl amide, alkyl nitrile, amino acid and N-heterocyclic alkaloid compounds
316 (Laskin et al., 2009). These compounds spread separately in two parts in molecular corridors. Some
317 compounds are assembled in the upper left space bounded by $\log_{10}C_0 > 0 \mu\text{g m}^{-3}$ and $M < 300 \text{ g}$

318 mol⁻¹. A part of these compounds may be a consequence of oxidative fragmentation or thermal
319 decomposition. Compounds clustered in the lower right space are CHON compounds with molar
320 mass higher than 300 g mol⁻¹ covering the range from LVOC to ELVOC.

321 More than two hundred N-containing compounds were identified at the Mt. Sonnblick (Fig. 6c;
322 Holzinger et al., 2010). Less oxidized N-containing organic compounds could be formed through
323 reactions transforming carbonyls into imines or reactions of NO with organic peroxy radicals
324 (O'Brien et al., 2014). Highly oxidized organonitrates (O:C>1) were suggested to be formed by
325 nitrate radical chemistry (Holzinger et al., 2010). Many highly oxidized N-containing compounds
326 with a range of O:C ratios from 1 to 2 were observed in fog (Fig. 6d; Mazzoleni et al., 2010), cloud
327 (Fig. 6e; Zhao et al., 2013), rain in New Jersey (Fig. 6f; Altieri et al., 2009a, 2009b) and Bermuda
328 (Fig. 6g; Altieri et al., 2012). Aqueous-phase processing can form a variety of highly-functionalized
329 nitrated organic compounds including organonitrates, hydroxynitrates, carbonyl nitrates and
330 dinitrates (Zhao et al., 2013). Reduced nitrogen compounds were also identified in atmospheric
331 water, mainly occupying the space close to the alkane line.

332 Figure 6h shows N-containing compounds found in the secondhand and thirdhand tobacco
333 smoke. Nitrosamines were found in third-hand smoke hazards when the residual nicotine reacts with
334 HONO (Sleiman et al., 2010b). Similar to the trend of CHO compounds in the molecular corridors
335 (Fig. 5h), N-containing compounds also mainly occupy the region close to the origin of the
336 molecular corridor. Some high molar mass N-containing compounds (*m/z* 400–500) were also
337 detected, but their elemental compositions and structures have not been identified (Sleiman et al.,
338 2010a).

339 Figure 7 shows S-containing compounds plotted in the molecular corridor. Organosulfate and
340 nitroxy-organosulfate were frequently identified in fine aerosols especially in urban areas including
341 Shanghai (Ma et al., 2014; Tao et al., 2014) and Guangzhou (Lin et al., 2012) in China, Taipei (Lin
342 et al., 2012), Lahore in Pakistan (Stone et al., 2012), Bakersfield (O'Brien et al., 2014) and Los
343 Angeles (Tao et al., 2014) in the U.S. as shown in Fig. 7a. Most of them are LVOC or ELVOC with

344 O:C ratio higher than 0.8 and molar mass in 200 – 400 g mol⁻¹. Some uncommon organosulfates
345 with higher molar mass but a lower degree of oxidation were found in Shanghai and long-chain
346 alkanes from vehicle emissions were suggested to be their precursors (Tao et al., 2014). Compared
347 to the organosulfates identified in urban areas, oxygenated sulfur-containing compounds
348 characterized at the Mt. Sonnblick have a relatively lower O:C ratio (~0.5 in an average) and molar
349 mass (mostly less than 250 g mol⁻¹) and higher volatility (IVOC or SVOC) (Fig. 7b). Similar to
350 highly oxidized N-containing compounds observed in fog, cloud and rain, S-containing highly
351 oxidized compounds including functionalized (nitro- and nitrooxy-) organosulfates were formed in
352 atmospheric water (Fig. 7c–f), which locate close to the sugar alcohol line in the range of LVOC
353 and ELVOC. Compounds close to the alkane line are mostly reduced sulfur compounds, e.g.,
354 aromatic structures containing only one S and one O, which may be emitted from primary sources.

355 Figure 8 summarizes the molecular corridor for amine, organonitrate, organosulfate, nitroxy
356 organosulfate and reduced sulfur compounds. The small markers are compounds identified in the
357 studies included in Fig. 6 & 7. Among these species, nitroxy-organosulfates have the highest O:C
358 ratio (> 0.9) and the lowest volatility falling into the ELVOC group with molar mass up to 400 g
359 mol⁻¹. Organosulfates and organonitrates have an O:C ratio generally higher than 0.7, covering the
360 range of IVOC to ELVOC with a broad molar mass range (100 – 600 g mol⁻¹) to occupy the high
361 O:C corridor. Note that there exists a homologous series of organosulfates with molar mass between
362 400 – 600 g mol⁻¹ and $\log_{10}(C_0) < -10$, which appear to have lower dlog C_0/dM values. These
363 compounds, e.g., C₁₇H₁₈O₁₆S₁, C₁₈H₂₀O₁₆S₁, and C₁₉H₂₂O₁₆S₁, were found in the cloud water and
364 their formation may be due to esterification of hydroxyl groups with sulfuric acid or acid-catalyzed
365 reactions of epoxides (Zhao et al., 2013). Reduced sulfur compounds have low O:C ratio (< 0.4) and
366 are located close to the alkane line. Amine and N-heterocyclic alkaloid compounds found during
367 new particle formation and biomass burning have the lowest O:C ratio and molar mass and the
368 highest volatility (in VOC and IVOC groups), following the low O:C corridor.

369

370 **5. Summary and conclusions**

371 From the analysis of measured OA locating into the molecular corridor, we can conclude that
372 the molecular corridor characterized by molar mass, saturation mass concentration, and O:C ratio
373 has successfully grasped the properties of organic compounds from different sources and formed in
374 various atmospheric conditions. Figure 9 shows the trend of observed organic compounds with
375 surrogate compounds with the mean values of molar mass, saturation mass concentration, and O:C
376 ratio derived from every observation event. The symbol size is scaled with the ratio of the number
377 of compound in each class (e.g., CH, CHO, CHON, CHONS) to the total number of compounds in
378 each observation.

379 OA in indoor environments have relatively lower molar mass and higher volatility, mainly
380 occupying the space close to the origin of the molecular corridor. Outdoor OA are constrained to a
381 corridor in the range of IVOC – LVOC with a molar mass of up to ~400 g mol⁻¹. Atmospheric water
382 of fog, cloud and rain droplets often contain many highly-oxygenated, high molar-mass, and low-
383 volatility compounds, extending to a wide space with higher molar mass and lower volatility.
384 Molecular corridors are a useful framework for analysis and interpretation of measurements by a
385 high-resolution mass spectrometer to visualize distribution of organic compounds providing insights
386 into the evolution of OA properties.

387 Explicit consideration of molar mass in an OA model would also be useful in inferring particle
388 phase state (liquid vs. semisolid vs. amorphous solid), as the molar mass correlates with the glass
389 transition temperature of organic compounds (Koop et al., 2011). The phase state has been shown to
390 affect various gas-particle interactions including heterogeneous and multiphase chemistry, SOA
391 formation and evolution as well as activation to cloud droplets and ice crystals (Pöschl and Shiraiwa,
392 2015 and references therein). Molecular corridors may serve as a basis for better treatment of SOA
393 properties and interpretation of model outputs in detailed SOA models (e.g., Shiraiwa et al., 2012;
394 Cappa et al., 2013; Roldin et al., 2014; Zaveri et al., 2014) as well as for compact representation of
395 OA formation and evolution in regional and global models of climate and air quality.

396 **Acknowledgements**

397 YL was supported by the Lindau Fellowship (Project No.: GZ 1116), granted by the Sino-German
398 Science Center. This work was supported by the Max Planck Society and the National Natural
399 Science Foundation of China (Grant No. 41405121). The authors gratefully acknowledge Lynn
400 Mazzoleni (Michigan Technological University), Alexander Laskin (Pacific Northwest National
401 Laboratory), Rupert Holzinger (Utrecht University), Neil Donahue (Carnegie Mellon University),
402 Thomas Mentel (Research Center Jülich), Frank Wania (University of Toronto Scarborough), Yiyi
403 Wei (Texas Tech University), Thomas Berkemeier (Max Planck Institute for Chemistry), Pascale
404 Lakey (Max Planck Institute for Chemistry) and John Seinfeld (Caltech) for stimulating discussions.
405 We thank Ulrich Krieger (ETH Zurich) and two anonymous referees for useful comments.

406

407 **References**

- 408 Ahmadov, R., McKeen, S. A., Robinson, A. L., Bahreini, R., Middlebrook, A. M., de Gouw, J. A.,
409 Meagher, J., Hsie, E.-Y., Edgerton, E., Shaw, S., and Trainer, M.: A volatility basis set model
410 for summertime secondary organic aerosols over the eastern United States in 2006, *J. Geophys.*
411 *Res.*, 117, D06301, doi:10.1029/2011JD016831, 2012.
- 412 Altieri, K. E., Seitzinger, S. P., Clalton, A. G., Trupin, B. J., Klein, G. C., and Marshall, A. G.:
413 Oligomers fromed through in-cloud methylglyoxal reactions: chemical composition, properties,
414 and mechanisms investigated by ultra-high resolution FT-ICR mass spectrometry, *Atmos.*
415 *Environ.*, 42, 1476-1490, 2008.
- 416 Altieri, K. E., Turpin, B. J., and Seitzinger, S. P.: Composition of dissolved organic nitrogen in
417 continental precipitation investigated by ultra-high resolution FT-ICR mass spectrometry,
418 *Environ. Sci. Technol.*, 43, 6950-6955, 2009a.
- 419 Altieri, K. E., Turpin, B. J., and Seitzinger, S. P.: Oligomers, organosulfates, and nitrooxy
420 organosulfates in rainwater identified by ultra-high resolution electrospray ionization FT-ICR
421 mass spectrometry, *Atmos. Chem. Phys.*, 9, 2533-2542, 2009b.

- 422 Altieri, K. E., Hastings, M. G., Peters, A. J., and Sigman, D. M.: Molecular characterization of
423 water soluble organic nitrogen in marine rainwater by ultra-high resolution electrospray
424 ionization mass spectrometry, *Atmos. Chem. Phys.*, 12, 3557-3571, 2012.
- 425 Barley, M. H., and McFiggans, G.: The critical assessment of vapour pressure estimation methods
426 for use in modelling the formation of atmospheric organic aerosol, *Atmos. Chem. Phys.*, 10,
427 749-767, 2010.
- 428 Bilde, M., Barsanti, K., Booth, M., Cappa, C. D., Donahue, N. M., Emanuelsson, E. U., McFiggans,
429 G., Krieger, U. K., Marcolli, C., Topping, D., Ziemann, P., Barley, M., Clegg, S.,
430 Dennis-Smither, B., Hallquist, M., Hallquist, Å. M., Khlystov, A., Kulmala, M., Mogensen, D.,
431 Percival, C. J., Pope, F., Reid, J. P., Ribeiro da Silva, M. A. V., Rosenoern, T., Salo, K.,
432 Soonsin, V. P., Yli-Juuti, T., Prisle, N. L., Pagels, J., Rarey, J., Zardini, A. A., and Riipinen, I.:
433 Saturation vapor pressures and transition enthalpies of low-volatility organic molecules of
434 atmospheric relevance: from dicarboxylic acids to complex mixtures, *Chem. Rev.*, 115,
435 4115-4156, 2015.
- 436 Boyd, C. M., Sanchez, J., Xu, L., Eugene, A. J., Nah, T., Tuet, W. Y., Guzman, M. I., and Ng, N. L.:
437 Secondary organic aerosol formation from the β -pinene+NO₃ system: effect of humidity and
438 peroxy radical fate, *Atmos. Chem. Phys.*, 15, 7497-7522, 2015.
- 439 Cappa, C. D., and Jimenez, J. L.: Quantitative estimates of the volatility of ambient organic aerosol,
440 *Atmos. Chem. Phys.*, 10, 5409-5424, 2010.
- 441 Cappa, C. D., and Wilson, K. R.: Multi-generation gas-phase oxidation, equilibrium partitioning,
442 and the formation and evolution of secondary organic aerosol, *Atmos. Chem. Phys.*, 12,
443 9505-9528, 2012.
- 444 Cappa, C. D., Zhang, X., Loza, C. L., Craven, J. S., Yee, L. D., and Seinfeld, J. H.: Application of
445 the Statistical Oxidation Model (SOM) to secondary organic aerosol formation from
446 photooxidation of C₁₂ alkanes, *Atmos. Chem. Phys.*, 13, 1591-1606, 2013.

- 447 Carlton, A. G., and Turpin, B. J.: Particle partitioning potential of organic compounds is highest in
448 the Eastern US and driven by anthropogenic water, *Atmos. Chem. Phys.*, 13, 10203-10214,
449 2013.
- 450 Chan, M. N., Nah, T., and Wilson, K. R.: Real time in situ chemical characterization of sub-micron
451 organic aerosols using Direct Analysis in Real Time mass spectrometry (DART-MS): the
452 effect of aerosol size and volatility, *Analyst*, 138, 3749-3757, 2013.
- 453 Clegg, S. L., Kleeman, M. J., Griffin, R. J., and Seinfeld, J. H.: Effects of uncertainties in the
454 thermodynamic properties of aerosol components in an air quality model—Part 2: Predictions
455 of the vapour pressures of organic compounds, *Atmos. Chem. Phys.*, 8, 1087-1103, 2008.
- 456 Compernolle, S., Ceulemans, K., and Muller, J. F.: EVAPORATION: a new vapour pressure
457 estimation method for organic molecules including non-additivity and intramolecular
458 interactions, *Atmos. Chem. Phys.*, 11, 9431-9450, 2011.
- 459 Crounse, J. D., Nielsen, L. B., Jorgensen, S., Kjaergaard, H. G., and Wennberg, P. O.: Autoxidation
460 of organic compounds in the atmosphere, *J. Phys. Chem. Lett.*, 4, 3513-3520, 2013.
- 461 Daumit, K. E., Carrasquillo, A. J., Hunter, J. F., and Kroll, J. H.: Laboratory studies of the
462 aqueous-phase oxidation of polyols: submicron particles vs. bulk aqueous solution, *Atmos.*
463 *Chem. Phys.*, 14, 10773-10784, 2014.
- 464 Destaillats, H., Singer, B. C., Lee, S. K., and Gundel, L. A.: Effect of ozone on nicotine desorption
465 from model surfaces: evidence for heterogeneous Chemistry, *Environ. Sci. Technol.*, 40,
466 1799-1805, 2006.
- 467 Donahue, N. M., Robinson, A. L., Stanier, C. O., and Pandis, S. N.: Coupled partitioning, dilution,
468 and chemical aging of semivolatile organics, *Environ. Sci. Technol.*, 40, 2635-2643, 2006.
- 469 Donahue, N. M., Epstein, S. A., Pandis, S. N., and Robinson, A. L.: A two-dimensional volatility
470 basis set: 1. organic-aerosol mixing thermodynamics, *Atmos. Chem. Phys.*, 11, 3303-3318,
471 2011.

- 472 Donahue, N. M., Kroll, J. H., Pandis, S. N., and Robinson, A. L.: A two-dimensional volatility basis
473 set – Part2: Diagnostics of organic-aerosol evolution, *Atmos. Chem. Phys.*, 12, 615-634, 2012.
- 474 Donahue, N. M., Robinson, A. L., Trump, E. R., Riipinen, I., and Kroll, J. H.: Volatility and aging
475 of atmospheric organic aerosol, in: *Atmospheric and Aerosol Chemistry*, edited by: McNeill, V.
476 F., and Ariya, P. A., *Topics in Current Chemistry*, 97-143, 2014.
- 477 Ehn, M., Junninen, H., Petäjä, T., Kurtén, T., Kerminen, V. M., Schobesberger, S., Manninen, H. E.,
478 Ortega, I. K., Vehkamäki, H., Kulmala, M., and Worsnop, D. R.: Composition and temporal
479 behavior of ambient ions in the boreal forest, *Atmos. Chem. Phys.*, 10, 8513-8530, 2010.
- 480 Ehn, M., Kleist, E., Junninen, H., Petäjä, T., Lönn, G., Schobesberger, S., Dal Maso, M., Trimborn,
481 A., Kulmala, M., Worsnop, D. R., Wahner, A., Wildt, J., and Mentel, T. F.: Gas phase
482 formation of extremely oxidized pinene reaction products in chamber and ambient air, *Atmos.*
483 *Chem. Phys.*, 12, 5113-5127, 2012.
- 484 Ehn, M., Thornton, J. A., Kleist, E., Sipila, M., Junninen, H., Pullinen, I., Springer, M., Rubach, F.,
485 Tillmann, R., Lee, B., Lopez-Hilfiker, F., Andres, S., Acir, I. H., Rissanen, M., Jokinen, T.,
486 Schobesberger, S., Kangasluoma, J., Kontkanen, J., Nieminen, T., Kurten, T., Nielsen, L. B.,
487 Jorgensen, S., Kjaergaard, H. G., Canagaratna, M., Dal Maso, M., Berndt, T., Petaja, T.,
488 Wahner, A., Kerminen, V. M., Kulmala, M., Worsnop, D. R., Wildt, J., and Mentel, T. F.: A
489 large source of low-volatility secondary organic aerosol, *Nature*, 506, 476-479, 2014.
- 490 Epstein, S. A., Riipinen, I., and Donahue, N. M.: A semiempirical correlation between enthalpy of
491 vaporization and saturation concentration for organic aerosol, *Environ. Sci. Technol.*, 44,
492 743-748, 2010.
- 493 Erupe, M. E., Viggiano, A. A., and Lee, S.-H.: The effect of trimethylamine on atmospheric
494 nucleation involving H_2SO_4 , *Atmos. Chem. Phys.*, 11, 4767-4775, 2011.
- 495 Ervens, B.: Modeling the processing of aerosol and trace gases in clouds and fogs, *Chem. Rev.*, 115,
496 4157-4198, 2015.

- 497 Ervens, B., Turpin, B. J., and Weber, R. J.: Secondary organic aerosol formation in cloud droplets
498 and aqueous particles (aqSOA): a review of laboratory, field and model studies, *Atmos. Chem.*
499 *Phys.*, 11, 11069-11102, 2011.
- 500 Farmer, D. K., Matsunaga, A., Docherty, K. S., Surratt, J. D., Seinfeld, J. H., Ziemann, P. J., and
501 Jimenez, J. L.: Response of an aerosol mass spectrometer to organonitrates and organosulfates
502 and implications for atmospheric chemistry, *P. Natl. Acad. Sci. USA*, 107, 6670-6675, 2010.
- 503 Fry, J. L., Draper, D. C., Zarzana, K. J., Campuzano-Jost, P., Day, D. A., Jimenez, J. L., Brown, S.
504 S., Cohen, R. C., Kaser, L., Hansel, A., cappellin, L., Karl, T., Hodzic Roux, A., Turnipseed,
505 A., cantrell, C., Lefer, B. L., and Grossberg, N.: Observations of gas- and aerosol-phase
506 organic nitrates at BEACHON-RoMBAS 2011, *Atmos. Chem. Phys.*, 13, 8585-8605, 2013.
- 507 Fuzzi, S., Baltensperger, U., Carslaw, K., Decesari, S., Denier van der Gon, H., Facchini, M. C.,
508 Fowler, D., Koren, I., Langford, B., Lohmann, U., Nemitz, E., Pandis, S., Riipinen, I., Rudich,
509 Y., Schaap, M., Slowik, J. G., Spracklen, D. V., Vignati, E., Wild, M., Williams, M., and
510 Gilardoni, S.: Particulate matter, air quality and climate: lessons learned and future needs,
511 *Atmos. Chem. Phys.*, 15, 8217-8299, 2015.
- 512 Gómez-González, Y., Wang, W., Vermeylen, R., Chi, X., Neirynck, J., Janssens, I. A., Maenhaut,
513 W., and Claeys, M.: Chemical characterisation of atmospheric aerosols during a 2007 summer
514 field campaign at Brasschaat, Belgium: sources and source processes of biogenic secondary
515 organic aerosol, *Atmos. Chem. Phys.*, 12, 125-138, 2012.
- 516 Hamilton, J. F., Baeza-Romero, M. T., Finessi, E., Rickard, A. R., Healy, R. M., Peppe, S., Adams,
517 T. J., Daniels, M. J. S., Ball, S. M., Goodall, I. C. A., Monks, P. S., Borrás, E., and Muñoz, A.:
518 Online and offline mass spectrometric study of the impact of oxidation and ageing on glyoxal
519 chemistry and uptake onto ammonium sulfate aerosols, *Faraday Discuss.*, 165, 447-472, 2013.
- 520 Hallquist, M., Wenger, J., Baltensperger, U., Rudich, Y., Simpson, D., Claeys, M., Dommen, J.,
521 Donahue, N., George, C., and Goldstein, A.: The formation, properties and impact of

- 522 secondary organic aerosol: current and emerging issues, *Atmos. Chem. Phys.*, 9, 5155-5236,
523 2009.
- 524 Hayes, P. L., Carlton, A. G., Baker, K. R., Ahmadov, R., Washenfelder, R. A., Alvarez, S.,
525 Rappenglück, B., Gilman, J. B., Kuster, W. C., de Gouw, J. A., Zotter, P., Prévôt, A. S. H.,
526 Szidat, S., Kleindienst, T. E., Offenberg, J. H., Ma, P. K., and Jimenez, J. L.: Modeling the
527 formation and aging of secondary organic aerosols in Los Angeles during CalNex 2010, *Atmos.*
528 *Chem. Phys.*, 15, 5773-5801, 2015.
- 529 Heald, C. L., Kroll, J. H., Jimenez, J. L., Docherty, K. S., DeCarlo, P. F., Aiken, A. C., Chen, Q.,
530 Martin, S. T., Farmer, D. K., and Artaxo, P.: A simplified description of the evolution of
531 organic aerosol composition in the atmosphere, *Geophys. Res. Lett.*, 37,
532 doi:10.1029/2010gl042737, 2010.
- 533 Holzinger, R., Goldstein, A. H., Hayes, P. L., Jimenez, J. L., and Timkovsky, J.: Chemical evolution
534 of organic aerosol in Los Angeles during the CalNex 2010 study, *Atmos. Chem. Phys.*, 13,
535 10125-10141, 2013.
- 536 Holzinger, R., Kasper-Giebl, A., Staudinger, M., Schauer, G., and Röckmann, T.: Analysis of the
537 chemical composition of organic aerosol at the Mt. Sonnblick observatory using a novel high
538 mass resolution thermal-desorption proton-transfer-reaction mass-spectrometer
539 (hr-TD-PTR-MS), *Atmos. Chem. Phys.*, 10, 10111-10128, 2010.
- 540 Huang, R. J., Zhang, Y. L., Bozzetti, C., Ho, K. F., Cao, J. J., Han, Y. M., Daellenbach, K. R.,
541 Slowik, J. G., Platt, S. M., Canonaco, F., Zotter, P., Wolf, R., Pieber, S. M., Bruns, E. A.,
542 Crippa, M., Ciarelli, G., Piazzalunga, A., Schwikowski, M., Abbaszade, G., Schnelle-Kreis, J.,
543 Zimmermann, R., An, Z. S., Szidat, S., Baltensperger, U., El Haddad, I., and Prevot, A. S. H.:
544 High secondary aerosol contribution to particulate pollution during haze events in China,
545 *Nature*, 514, 218-222, 2014.

- 546 Huisman, A. J., Krieger, U. K., Zuend, A., Marcolli, C., and Peter, T.: Vapor pressures of
547 substituted polycarboxylic acids are much lower than previously reported, *Atmos. Chem. Phys.*,
548 13, 6647-6662, 2013.
- 549 Iinuma, Y., Muller, C., Berndt, T., Boge, O., Claeys, M., and Herrmann, H.: Evidence for the
550 existence of organosulfates from beta-pinene ozonolysis in ambient secondary organic aerosol,
551 *Environ. Sci. Technol.*, 41, 6678-6683, 2007.
- 552 Jathar, S. H., Miracolo, M. A., Presto, A. A., Donahue, N. M., Adams, P. J., and Robinson, A. L.:
553 Modeling the formation and properties of traditional and non-traditional secondary organic
554 aerosol: problem formulation and application to aircraft exhaust, *Atmos. Chem. Phys.*, 12,
555 9025-9040, 2012.
- 556 Jimenez, J. L., Canagaratna, M. R., Donahue, N. M., Prevot, A. S. H., Zhang, Q., Kroll, J. H.,
557 DeCarlo, P. F., Allan, J. D., Coe, H., Ng, N. L., Aiken, A. C., Docherty, K. S., Ulbrich, I. M.,
558 Grieshop, A. P., Robinson, A. L., Duplissy, J., Smith, J. D., Wilson, K. R., Lanz, V. A.,
559 Hueglin, C., Sun, Y. L., Tian, J., Laaksonen, A., Raatikainen, T., Rautiainen, J., Vaattovaara,
560 P., Ehn, M., Kulmala, M., Tomlinson, J. M., Collins, D. R., Cubison, M. J., Dunlea, E. J.,
561 Huffman, J. A., Onasch, T. B., Alfarra, M. R., Williams, P. I., Bower, K., Kondo, Y.,
562 Schneider, J., Drewnick, F., Borrmann, S., Weimer, S., Demerjian, K., Salcedo, D., Cottrell, L.,
563 Griffin, R., Takami, A., Miyoshi, T., Hatakeyama, S., Shimono, A., Sun, J. Y., Zhang, Y. M.,
564 Dzepina, K., Kimmel, J. R., Sueper, D., Jayne, J. T., Herndon, S. C., Trimborn, A. M.,
565 Williams, L. R., Wood, E. C., Middlebrook, A. M., Kolb, C. E., Baltensperger, U., and
566 Worsnop, D. R.: Evolution of Organic Aerosols in the Atmosphere, *Science*, 326, 1525-1529,
567 2009.
- 568 Kahnt, A., Behrouzi, S., Vermeylen, R., Shalamzari, M. S., Vercauteren, J., Roekens, E., Claeys, M.,
569 and Maenhaut, W.: One-year study of nitro-organic compounds and their relation to wood
570 burning in PM₁₀ aerosol from a rural site in Belgium, *Atmos. Environ.*, 81, 561-568, 2013.

- 571 Kampf, C. J., Bonn, B., and Hoffmann, T.: Development and validation of a selective
572 HPLC-ESI-MS/MS method for the quantification of glyoxal and methylglyoxal in atmospheric
573 aerosols (PM_{2.5}), *Anal. Bioanal. Chem.*, 401, 3115-3124, 2011.
- 574 Kanakidou, M., Seinfeld, J., Pandis, S., Barnes, I., Dentener, F., Facchini, M., Dingenen, R. V.,
575 Ervens, B., Nenes, A., and Nielsen, C.: Organic aerosol and global climate modelling: a review,
576 *Atmos. Chem. Phys.*, 5, 1053-1123, 2005.
- 577 Kitanovski, Z., Grgić, I., Vermeylen, R., Claeys, M., and Maenhaut, W.: Liquid chromatography
578 tandem mass spectrometry method for characterization of monoaromatic nitro-compounds in
579 atmospheric particulate matter, *J. Chromatogr.*, A, 1268, 35-43, 2012.
- 580 Koop, T., Bookhold, J., Shiraiwa, M., and Pöschl, U.: Glass transition and phase state of organic
581 compounds: dependency on molecular properties and implications for secondary organic
582 aerosols in the atmosphere, *Phys. Chem. Chem. Phys.*, 13, 19238-19255, 2011.
- 583 Kourtchev, I., O'Connor, I. P., Giorio, C., Fuller, S. J., Kristensen, K., Maenhaut, W., Wenger, J. C.,
584 Sodeau, J. R., Glasius, M., and Kalberer, M.: Effects of anthropogenic emissions on the
585 molecular composition of urban organic aerosols: An ultrahigh resolution mass spectrometry
586 study, *Atmos. Environ.*, 89, 525-532, 2014.
- 587 Krieger, U. K., Marcolli, C., and Reid, J. P.: Exploring the complexity of aerosol particle properties
588 and processes using single particle techniques, *Chem. Soc. Rev.*, 41, 6631-6662, 2012.
- 589 Kroll, J. H., Donahue, N. M., Jimenez, J. L., Kessler, S. H., Canagaratna, M. R., Wilson, K. R.,
590 Altieri, K. E., Mazzoleni, L. R., Wozniak, A. S., Bluhm, H., Mysak, E. R., Smith, J. D., Kolb,
591 C. E., and Worsnop, D. R.: Carbon oxidation state as a metric for describing the chemistry of
592 atmospheric organic aerosol, *Nature Chemistry*, 3, 133-139, 2011.
- 593 Kroll, J. H., and Seinfeld, J. H.: Chemistry of secondary organic aerosol: Formation and evolution
594 of low-volatility organics in the atmosphere, *Atmos. Environ.*, 42, 3593-3624, 2008.
- 595 Kulmala, M., Kontkanen, J., Junninen, H., Lehtipalo, K., Manninen, H. E., Nieminen, T., Petäjä, T.,
596 Sipilä, M., Schobesberger, S., Rantala, P., Franchin, A., Jokinen, T., Järvinen, E., Äijälä, M.,

- 597 Kangasluoma, J., Hakala, J., Aalto, P. P., Paasonen, P., Mikkilä, J., Vanhanen, J., Aalto, J.,
598 Hakala, H., Makkonen, U., Ruuskanen, T., Mauldin III, R. L., Duplissy, J., Vehkamäki, H.,
599 Bäck, J., Kortelainen, A., Riipinen, I., Kurtén, T., Johnston, M. V., Smith, J. M., Ehn, M.,
600 Mentel, Th. F., Lehtinen, K. E., Laaksonen, A., Kerminen, V.-M., and Worsnop, D. R.: Direct
601 observation of atmospheric aerosol nucleation, *Science*, 339, 943–946, 2013.
- 602 Kulmala, M., Petäjä, T., Ehn, M., Thornton, J., Sipilä, M., Worsnop, D. R., and Kerminen, V.-M.:
603 Chemistry of atmospheric nucleation: on the recent advances on precursor characterization and
604 atmospheric cluster composition in connection with atmospheric new particle formation, *Annu.
605 Rev. Phys. Chem.*, 65, 21-37, 2014.
- 606 Kundu, S., Quraishi, T. A., Yu, G., Suarez, C., Keutsch, F. N., and Stone, E. A.: Evidence and
607 quantitation of aromatic organosulfates in ambient aerosols in Lahore, Pakistan, *Atmos. Chem.
608 Phys.*, 13, 4865-4875, 2013.
- 609 Lane, T. E., Donahue, N. M., and Pandis, S. N.: Simulating secondary organic aerosol formation
610 using the volatility basis-set approach in a chemical transport model, *Atmos. Environ.*, 42,
611 7439-7451, 2008.
- 612 Laskin, A., Laskin, J., and Nizkorodov, S. A.: Mass spectrometric approaches for chemical
613 characterisation of atmospheric aerosols: critical review of the most recent advances, *Environ.
614 Chem.*, 9, 163-189, 2012.
- 615 Laskin, A., Smith, J. S., and Laskin, J.: Molecular Characterization of Nitrogen-Containing Organic
616 Compounds in Biomass Burning Aerosols Using High-Resolution Mass Spectrometry, *Environ.
617 Sci. Technol.*, 43, 3764-3771, 2009.
- 618 Lim, Y. B., Tan, Y., Perri, M. J., Seitzinger, S. P., and Turpin, B. J.: Aqueous chemistry and its role
619 in secondary organic aerosol (SOA) formation, *Atmos. Chem. Phys.*, 10, 10521-10539, 2010.
- 620 Lin, P., Yu, J., Engling, G., and Kalberer, M.: Organosulfates in humic-like substance fraction
621 isolated from aerosols at seven locations in East Asia: a study by ultra-high-resolution mass
622 spectrometry, *Environ. Sci. Technol.*, 46, 13118-13127, 2012.

- 623 Lobert, J. M., Scharffe, D. H., Hao, W. M., and Crutzen, P. J.: Importance of biomass burning in the
624 atmospheric budgets of nitrogen-containing gases, *Nature*, 346, 552-554, 1990.
- 625 Loukonen, V., Kurtén, T., Ortega, I. K., Vehkamäki, H., Pádua, A. A. H., Sellegri, K., and Kulmala,
626 M.: Enhancing effect of dimethylamine in sulfuric acid nucleation in the presence of water – a
627 computational study, *Atmos. Chem. Phys.*, 10, 4961-4974, 2010.
- 628 Lukács, H., Gelencsér, A., Hoffer, A., Kiss, G., Horváth, K., and Hartyán, Z.: Quantitative
629 assessment of organosulfates in size-segregated rural fine aerosol, *Atmos. Chem. Phys.*, 9,
630 231-238, 2009.
- 631 Lyman, W. J.: In: Environmental exposure from chemicals, Volume I., Neely, W. B. and Blau, G. E.
632 (eds), Boca Raton, FL: CRC Press, Inc., Chapter 2, 1985.
- 633 Lyman, W. J., Reehl, W. F., and Rosenblatt, D. H.: Handbook of chemical property estimation
634 methods, Washington, DC: American Chemical Society, Chapter 14, 1990.
- 635 Ma, Y., Xu, X., Song, W., Geng, F., and Wang, L.: Seasonal and diurnal variations of particulate
636 organosulfates in urban Shanghai, China, *Atmos. Environ.*, 85, 152-160, 2014.
- 637 Matsui, H., Koike, M., Kondo, Y., Takami, A., Fast, J. D., Kanaya, Y., and Takigawa, M.: Volatility
638 basis-set approach simulation of organic aerosol formation in East Asia: implications for
639 anthropogenic-biogenic interaction and controllable amounts, *Atmos. Chem. Phys.*, 14,
640 9513-9535, 2014.
- 641 Mazzoleni, L. R., Ehrmann, B. M., Shen, X. H., Marshall, A. G., and Collett, J. L.: Water-soluble
642 atmospheric organic matter in fog: exact masses and chemical formula identification by
643 ultrahigh-resolution Fourier transform ion cyclotron resonance mass spectrometry, *Environ.*
644 *Sci. Technol.*, 44, 3690-3697, 2010.
- 645 McNeill, V. F., Woo, J. L., Kim, D. D., Schwier, A. N., Wannell, N. J., Sumner, A. J. and Barakat, J.
646 M.: Aqueous-phase secondary organic aerosol and organosulfate formation in atmospheric
647 aerosols: a modeling study, *Environ. Sci. Technol.*, 46, 8075-8081, 2012.

- 648 Mead, R. N., Felix, J. D., Avery, G. B., Kieber, R. J., Willey, J. D., and Podgorski, D. C.:
649 Characterization of CHOS compounds in rainwater from continental and coastal storms by
650 ultrahigh resolution mass spectrometry, *Atmos. Environ.*, 105, 162-168, 2015.
- 651 Mentel, T. F., Springer, M., Ehn, M., Kleist, E., Pullinen, I., Kurtén, T., Rissanen, M., Wahner, A.,
652 and Wildt, J.: Formation of highly oxidized multifunctional compounds: autoxidation of
653 peroxy radicals formed in the ozonolysis of alkenes – deduced from structure-product
654 relationships, *Atmos. Chem. Phys.*, 15, 6745-6765, 2015.
- 655 Mentel, T. F., Wildt, J., Kiendler-Scharr, A., Kleist, E., Tillmann, R., Dal Maso, M., Fisseha, R.,
656 Hohaus, T., Spahn, H., Uerlings, R., Wegener, R., Griffiths, P. T., Dinar, E., Rudich, Y., and
657 Wahner, A.: Photochemical production of aerosols from real plant emissions, *Atmos. Chem.
658 Phys.*, 9, 4387-4406, 2009.
- 659 Morino, Y., Tanabe, K., Sato, K., and Ohara, T.: Secondary organic aerosol model intercomparision
660 based on secondary organic aerosol to odd oxygen ratio in Tokyo, *J. Geophys. Res. Atmos.*,
661 119, 13489-13505, 2014.
- 662 Murphy, B. N., Donahue, N. M., Fountoukis, C., Dall’Osto, M., O’Dowd, C., Kiendler-Scharr, A.,
663 and Pandis, S. N.: Functionalization and fragmentation during ambient organic aerosol aging:
664 application of the 2-D volatility basis set to field studies, *Atmos. Chem. Phys.*, 12,
665 10797-10816, 2012.
- 666 Murphy, B. N., Donahue, N. M., Robinson, A. L., and Pandis, S. N.: A naming convention for
667 atmospheric organic aerosol, *Atmos. Chem. Phys.*, 14, 5825-5839, 2014.
- 668 Murphy, B. N., and Pandis, S. N.: Simulating the formation of semivolatile primary and secondary
669 organic aerosol in a regional chemical transport model, *Environ. Sci. Technol.*, 43, 4722-4728,
670 2009.
- 671 Nizkorodov, S. A., Laskin, J., and Laskin, A.: Molecular chemistry of organic aerosols through the
672 application of high resolution mass spectrometry, *Phys. Chem. Chem. Phys.*, 13, 3612-3629,
673 2011.

- 674 Nozi ère, B., Kalberer, M., Claeys, M., Allan, J., D'Anna, B., Decesari, S., Finessi, E., Glasius, M.,
675 Grgić, I., Hamilton, J. F., Hoffmann, T., Iinuma, Y., Jaoui, M., Kahnt, A., Kampf, C. J., Kourtchev,
676 I., Maenhaut, W., Marsden, N., Saarikoski, S., Schnelle-Kreis, J., Surratt, J. D., Szidat, S.,
677 Szmigielski, R., and Wisthaler, A.: The molecular identification of organic compounds in the
678 atmosphere: state of the art and challenges, *Chem. Rev.*, 115, 3919-3983, 2015.
- 679 O'Brien, R. E., Laskin, A., Laskin, J., Rubitschun, C. L., Surratt, J. D., and Goldstein, A. H.: Molecular
680 characterization of S- and N-containing organic constituents in ambient aerosols by negative ion
681 mode high-resolution Nanospray Desorption Electrospray Ionization Mass spectrometry: CalNex
682 2010 field study, *J. Geophys. Res. Atmos.*, 119, 12706-12720, 2014.
- 683 Odum, J. R., Hoffmann, T., Bowman, F., Collins, D., Flagan, R. C., and Seinfeld, J. H.: Gas/particle
684 partitioning and secondary organic aerosol yields, *Environ. Sci. Technol.*, 30, 2580-2585,
685 1996.
- 686 O'Meara, S., Booth, A. M., Barley, M. H., Topping, D., and McFiggans, G.: An assessment of
687 vapour pressure estimation methods, *Phys. Chem. Chem. Phys.*, 16, 19453-19469, 2014.
- 688 Pankow, J. F.: An absorption-model of the gas aerosol partitioning involved in the formation of
689 secondary organic aerosol, *Atmos. Environ.*, 28, 189-193, 1994.
- 690 Pankow, J. F., and Barsanti, K. C.: The carbon number-polarity grid: A means to manage the
691 complexity of the mix of organic compounds when modeling atmospheric organic particulate
692 matter, *Atmos. Environ.*, 43, 2829-2835, 2009.
- 693 Pöschl, U., and Shiraiwa, M.: Multiphase chemistry at the atmosphere-biosphere interface
694 influencing climate and public health in the anthropocene, *Chem. Rev.*, 115, 4440-4475, 2015.
- 695 Reemtsma, T.: Determination of molecular formulas of natural organic matter molecules by (ultra-)
696 high-resolution mass spectrometry: status and needs, *J Chromatogr. A*, 1216, 3687-3701, 2009.
- 697 Riccobono, F., Schobesberger, S., Scott, C. E., Dommen, J., Ortega, I. K., Rondo, L., Almeida, J.,
698 Amorim, A., Bianchi, F., Breiten-lechner, M., David, A., Downard, A., Dunne, E. M., Duplissy,
699 J., Ehrhart, S., Flagan, R. C., Franchin, A., Hansel, A., Junninen, H., Kajos, M., Keskinen, H.,
700 Kupc, A., Kuerten, A., Kvashin, A. N., Laaksonen, A., Lehtipalo, K., Makhmutov, V., Mathot,

- 701 S., Nieminen, T., Onnela, A., Petaja, T., Praplan, A. P., Santos, F. D., Schallhart, S., Seinfeld, J.
702 H., Sipilä M., Spracklen, D. V., Stozhkov, Y., Stratmann, F., Tome, A., Tsagkogeorgas, G.,
703 Vaattovaara, P., Viisanenm Y., Vrtala, A., Wagner, P. E., Wein gartner, E., Wex, H., Wimmer,
704 D., Carslaw, K. S., Curtius, J., Donahue, N. M., Kirkby, J., Kulmala, M., Worsnop, D. R., and
705 Baltensperger, U.: Oxidation products of biogenic emissions contribute to nucleation of
706 atmospheric particles, *Science*, 344, 717–721, 2014.
- 707 Riipinen, I., Yli-Juuti, T., Pierce, J. R., Petaja, T., Worsnop, D. R., Kulmala, M., and Donahue, N.
708 M.: The contribution of organics to atmospheric nanoparticle growth, *Nature Geosci.*, 5, 453–
709 458, 2012.
- 710 Roldin, P., Eriksson, A. C., Nordin, E. Z., Hermansson, E., Mogensen, D., Rusanen, A., Boy, M.,
711 Swietlicki, E., Svenningsson, B., Zelenyuk, A., and Pagels, J.: Modelling non-equilibrium
712 secondary organic aerosol formation and evaporation with the aerosol dynamics, gas- and
713 particle-phase chemistry kinetic multilayer model ADCHAM, *Atmos. Chem. Phys.*, 14,
714 7953-7993, 2014.
- 715 Rollins, A. W., Browne, E. C., Min, K.-E., Pusede, S. E., Wooldridge, P. J., Gentner, D. R.,
716 Goldstein, A. H., Liu, S., Day, D. A., Russell, L. M., and Cohen, R. C.: Evidence for NO_x
717 control over nighttime SOA formation, *Science*, 337, 1210-1212, 2012.
- 718 Romero, F., and Oehme, M.: Organosulfates - A new component of humic-like substances in
719 atmospheric aerosols?, *J. Atmos. Chem.*, 52, 283-294, 2005.
- 720 Schmitt-Kopplin, P., Gelencsér, A., Dabek-Zlotorzynska, E., Kiss, G., Norbert, H., Harir, M., Hong,
721 Y., and Gebefügi, I.: Analysis of the unresolved organic fraction in atmospheric aerosols with
722 Ultrahigh-Resolution Mass Spectrometry and Nuclear Magnetic Resonance Spectroscopy:
723 organosulfates as photochemical smog constituents, *Anal. Chem.*, 82, 8017-8026, 2010.
- 724 Schobesberger, S., Junninen, H., Bianchi, F., Lonn, G., Ehn, M., Lehtipalo, K., Dommen, J., Ehrhart,
725 S., Ortega, I. K., Franchin, A., Nieminen, T., Riccobono, F., Hutterli, M., Duplissy, J., Almeida,
726 J., Amorim, A., Breitenlechner, M., Downard, A. J., Dunne, E. M., Flagan, R. C., Kajos, M.,

- 727 Keskinen, H., Kirkby, J., Kupc, A., Kurten, A., Kurten, T., Laaksonen, A., Mathot, S., Onnela,
728 A., Praplan, A. P., Rondo, L., Santos, F. D., Schallhart, S., Schnitzhofer, R., Sipila, M., Tome,
729 A., Tsagkogeorgas, G., Vehkamaki, H., Wimmer, D., Baltensperger, U., Carslaw, K. S.,
730 Curtius, J., Hansel, A., Petaja, T., Kulmala, M., Donahue, N. M., and Worsnop, D. R.:
731 Molecular understanding of atmospheric particle formation from sulfuric acid and large
732 oxidized organic molecules, *P. Natl. Acad. Sci. USA*, 110, 17223-17228, 2013.
- 733 Shiraiwa, M., Pfrang, C., Koop, T., and Pöschl, U.: Kinetic multi-layer model of gas-particle
734 interactions in aerosols and clouds (KM-GAP): linking condensation, evaporation and
735 chemical reactions of organics, oxidants and water, *Atmos. Chem. Phys.*, 12, 2777-2794, 2012.
- 736 Shiraiwa, M., Yee, L. D., Schilling, K. A., Loza, C. L., Craven, J. S., Zuend, A., Ziemann, P. J., and
737 Seinfeld, J. H.: Size distribution dynamics reveal particle-phase chemistry in organic aerosol
738 formation, *P. Natl. Acad. Sci. USA*, 110, 11746-11750, 2013a.
- 739 Shiraiwa, M., Zuend, A., Bertram, A. K., and Seinfeld, J. H.: Gas-particle partitioning of
740 atmospheric aerosols: interplay of physical state, non-ideal mixing and morphology, *Phys.
741 Chem. Chem. Phys.*, 15, 11441-11453, 2013b.
- 742 Shiraiwa, M., Berkemeier, T., Schilling-Fahnstock, K. A., Seinfeld, J. H., and Pöschl, U.:
743 Molecular corridors and kinetic regimes in the multiphase chemical evolution of secondary
744 organic aerosol, *Atmos. Chem. Phys.*, 14, 8323-8341, 2014.
- 745 Shrivastava, M., Fast, J., Easter, R., Gustafson Jr., W. I., Zaveri, R. A., Jimenez, J. L., Saide, P., and
746 Hodzic, A.: Modeling organic aerosols in a megacity: comparison of simple and complex
747 representations of the volatility basis set approach, *Atmos. Chem. Phys.*, 11, 6639-6662, 2011.
- 748 Simoneit, B. R. T.: Biomass burning - A review of organic tracers for smoke from incomplete
749 combustion, *Appl. Geochem.*, 17, 129-162, 2002.
- 750 Sleiman, M., Destaillats, H., Smith, J. D., Liu, C. L., Ahmed, M., Wilson, K. R., and Gundel, L. A.:
751 Secondary organic aerosol formation from ozone-initiated reactions with nicotine and
752 secondhand tobacco smoke, *Atmos. Environ.*, 44, 4191-4198, 2010a.

- 753 Sleiman, M., Gundel, L. A., Pankow, J. F., Jacob, P., Singer, B. C., and Destaillats, H.: Formation
754 of carcinogens indoors by surface-mediated reactions of nicotine with nitrous acid, leading to
755 potential thirdhand smoke hazards, *P. Natl. Acad. Sci. USA*, 107, 6576-6581, 2010b.
- 756 Smith, J. N., Barsanti, K. C., Friedli, H. R., Ehn, M., Kulmala, M., Collins, D. R., Scheckman, J. H.,
757 Williams, B. J., and McMurry, P. H.: Observations of aminium salts in atmospheric
758 nanoparticles and possible climatic implications, *P. Natl. Acad. Sci. USA*, 107, 6634-6639,
759 2010.
- 760 Staudt, S., Kundu, S., Lehmler, H.-J., He, X., Cui, T., Lin, Y.-H., Kristensen, K., Glasius, M.,
761 Zhang, X., Weber, R. J., Surratt, J. D., and Stone, E. A.: Aromatic organosulfates in
762 atmospheric aerosols: synthesis, characterization, and abundance, *Atmos. Environ.*, 94,
763 366-373, 2014.
- 764 Stone, E. A., Yang, L., Yu, L. E., and Rupakheit, M.: Characterization of organosulfates in
765 atmospheric aerosols at four Asian locations, *Atmos. Environ.*, 47, 323-329, 2012.
- 766 Sun, Y. L., Zhang, Q., Anastasio, C. and Sun, J.: Insights into secondary organic aerosol formed via
767 aqueous-phase reactions of phenolic compounds based on high resolution mass spectrometry,
768 *Atmos. Chem. Phys.*, 10, 4809-4822, 2010.
- 769 Surratt, J. D., Gomez-Gonzalez, Y., Chan, A. W. H., Vermeylen, R., Shahgholi, M., Kleindienst, T.
770 E., Edney, E. O., Offenberg, J. H., Lewandowski, M., Jaoui, M., Maenhaut, W., Claeys, M.,
771 Flagan, R. C., and Seinfeld, J. H.: Organosulfate formation in biogenic secondary organic
772 aerosol, *J. Phys. Chem. A*, 112, 8345-8378, 2008.
- 773 Surratt, J. D., Kroll, J. H., Kleindienst, T. E., Edney, E. O., Claeys, M., Sorooshian, A., Ng, N. L.,
774 Offenberg, J. H., Lewandowski, M., Jaoui, M., Flagan, R. C., and Seinfeld, J. H.: Evidence of
775 organosulfates in secondary organic aerosol, *Environ. Sci. Technol.*, 41, 517-527, 2007.
- 776 Tao, S., Lu, X., Levac, N., Bateman, A. P., Nguyen, T. B., Bones, D. L., Nizkorodov, S. A., Laskin,
777 J., Laskin, A., and Yang, X.: Molecular characterization of organosulfates in organic aerosols
778 from Shanghai and Los Angeles Urban Areas by Nanospray-Desorption Electrospray

- 779 Ionization High-Resolution Mass Spectrometry, Environ. Sci. Technol., 48, 10993-11001,
780 2014.
- 781 Tolocka, M. P., Jang, M., Ginter, J. M., Cox, F. J., Kamens, R. M., and Johnston, M. V.: Formation
782 of oligomers in secondary organic aerosol, Environ. Sci. Technol., 38, 1428-1434, 2004.
- 783 Tsimpidi, A. P., Karydis, V. A., Zavala, M., Lei, W., Molina, L., Ulbrich, I. M., Jimenez, J. L., and
784 Pandis, S. N.: Evaluation of the volatility basis-set approach for the simulation of organic
785 aerosol formation in the Mexico City metropolitan area, Atmos. Chem. Phys., 10, 525-546,
786 2010.
- 787 Tsimpidi, A. P., Karydis, V. A., Pozzer, A., Pandis, S. N., and Lelieveld, J.: ORACLE (v1.0):
788 module to simulate the organic aerosol composition and evolution in the atmosphere, Geosci.
789 Model Dev., 7, 3153-3172, 2014.
- 790 US EPA: Estimation Programs Interface SuiteTM for Microsoft Windows v4.1, United States
791 Environmental Protection Agency, Washington, DC, USA, 2015.
- 792 Wang, L., Khalizov, A. F., Zheng, J., Xu, W., Ma, Y., Lal, V., and Zhang, R.: Atmospheric
793 nanoparticles formed from heterogeneous reactions of organics, Nature Geosci., 3, 238-242,
794 2010.
- 795 Wania, F., Lei, Y. D., Wang, C., Abbatt, J. P. D., and Goss, K. U.: Novel methods for predicting
796 gas-particle partitioning during the formation of secondary organic aerosol, Atmos. Chem.
797 Phys., 14, 13189-13204, 2014.
- 798 Wania, F., Lei, Y. D., Wang, C., Abbatt, J. P. D., and Goss, K. U.: Using the chemical equilibrium
799 partitioning space to explore factors influencing the phase distribution of compounds involved
800 in secondary organic aerosol formation, Atmos. Chem. Phys., 15, 3395-3412, 2015.
- 801 Wei, Y. Y., Cao, T. T., and Thompson, J. E.: The chemical evolution & physical properties of
802 organic aerosol: A molecular structure based approach, Atmos. Environ., 62, 199-207, 2012.
- 803 Weschler, C. J.: Chemistry in indoor environments: 20 years of research, Indoor Air, 21, 205-218,
804 2011.

- 805 Wildt, J., Mentel, T. F., Kiendler-Scharr, A., Hoffmann, T., Andres, S., Ehn, M., Kleist, E., Müsgen,
806 P., Rohrer, F., Rudich, Y., Springer, M., Tillmann, R., and Wahner, A.: suppression of new
807 particle formation from monoterpene oxidation by NO_x, *Atmos. Chem. Phys.*, 14, 2789-2804,
808 2014.
- 809 Williams, B., Goldstein, A. H., Kreisberg, N. M., and Hering, S. V.: In situ measurements of
810 gas/particle-phase transitions for atmospheric semivolatile organic compounds, *P. Natl. Acad.
811 Sci. USA*, 107, 6676-6681, 2010.
- 812 Wisthaler, A., and Weschler, C. J.: Reactions of ozone with human skin lipids: Sources of carbonyls,
813 dicarbonyls, and hydroxycarbonyls in indoor air, *P. Natl. Acad. Sci. USA*, 107, 6568-6575,
814 2010.
- 815 Zaveri, R. A., Easter, R. C., Shilling, J. E., and Seinfeld, J. H.: Modeling kinetic partitioning of
816 secondary organic aerosol and size distribution dynamics: representing effects of volatility,
817 phase state, and particle-phase reaction, *Atmos. Chem. Phys.*, 14, 5153-5181, 2014.
- 818 Zhang, R., Khalizov, A., Wang, L., Hu, M., and Xu, W.: Nucleation and growth of nanoparticles in
819 the atmosphere, *Chem. Rev.*, 112, 1957-2011, 2011.
- 820 Zhang, R. Y., Wang, G. H., Guo, S., Zarnora, M. L., Ying, Q., Lin, Y., Wang, W. G., Hu, M., and
821 Wang, Y.: Formation of urban fine particulate matter, *Chem. Rev.*, 115, 3803-3855, 2015.
- 822 Zhang, X., and Seinfeld, J. H.: A functional group oxiation model (FGOM) for SOA formation and
823 aging, *Atmos. Chem. Phys.*, 13, 5907-5926, 2013.
- 824 Zhao, Y., Hallar, A. G., and Mazzoleni, L. R.: Atmospheric organic matter in clouds: exact masses
825 and molecular formula identification using ultrahigh-resolution FT-ICR mass spectrometry,
826 *Atmos. Chem. Phys.*, 13, 12343-12362, 2013.
- 827 Ziemann, P. J., and Atkinson, R.: Kinetics, products, and mechanisms of secondary organic aerosol
828 formation, *Chem. Soc. Rev.*, 19, 6582-6605, 2012.
- 829 Zuend, A., and Seinfeld, J. H.: Modeling the gas-particle partitioning of secondary organic aerosol:
830 the importance of liquid-liquid phase separation, *Atmos. Chem. Phys.*, 12, 3857-3882, 2012.

831 **Table 1.** Composition classes and the n_C^0 and b values for saturation mass concentration
 832 parameterizations obtained by least-squares optimization using the NCI database.

Classes	n_C^0	b_C	b_O	b_{CO}	b_N	b_S
CH	23.80	0.4861				
CHO	22.66	0.4481	1.656	-0.7790		
CHN	24.59	0.4066			0.9619	
CHON	24.13	0.3667	0.7732	-0.07790	1.114	
CHOS	24.06	0.3637	1.327	-0.3988		0.7579
CHONS	28.50	0.3848	1.011	0.2921	1.053	1.316

837

838

839

840

841

842

843

844

845

846

847

848

849

850

851

852

853

854

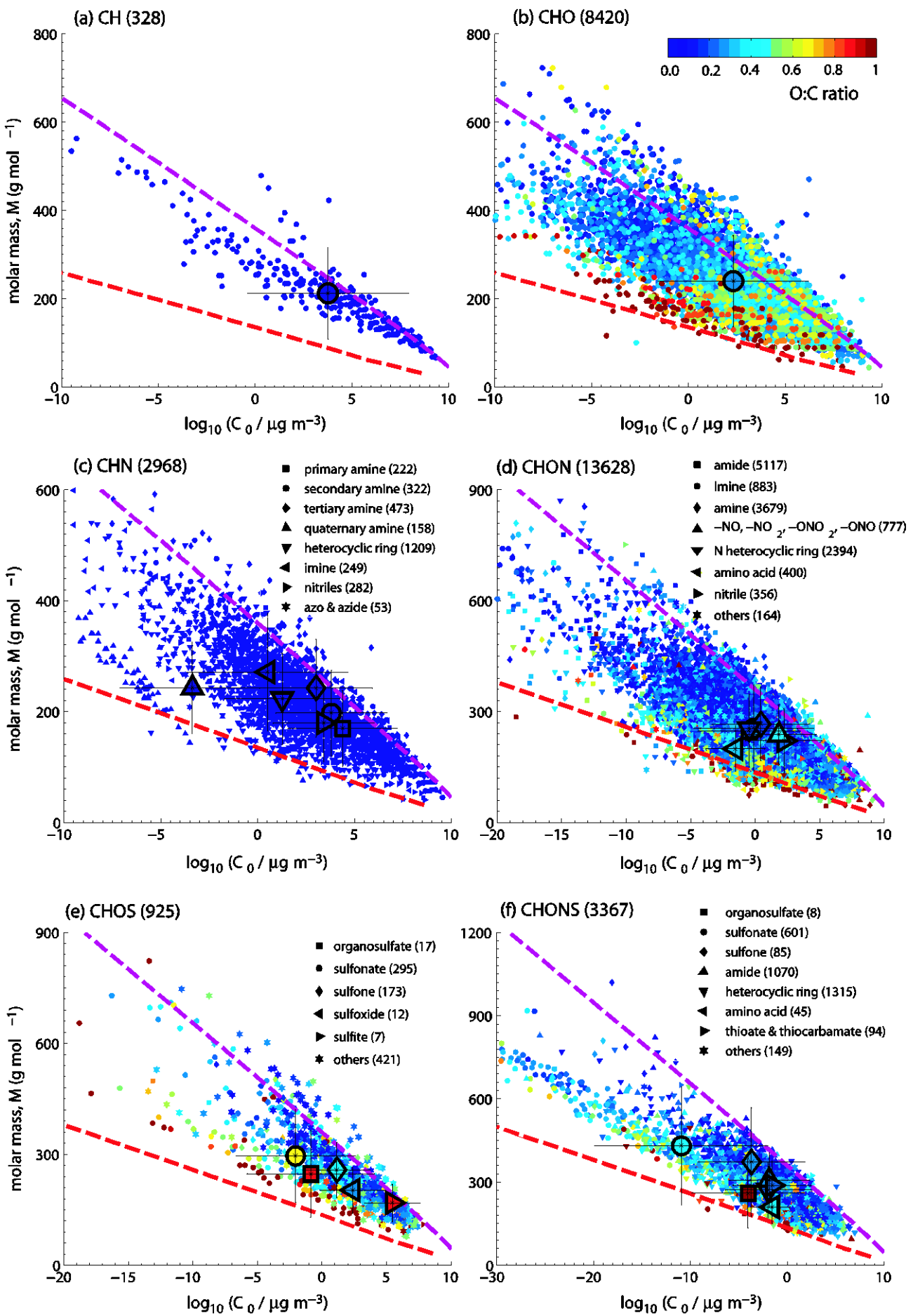
855

856

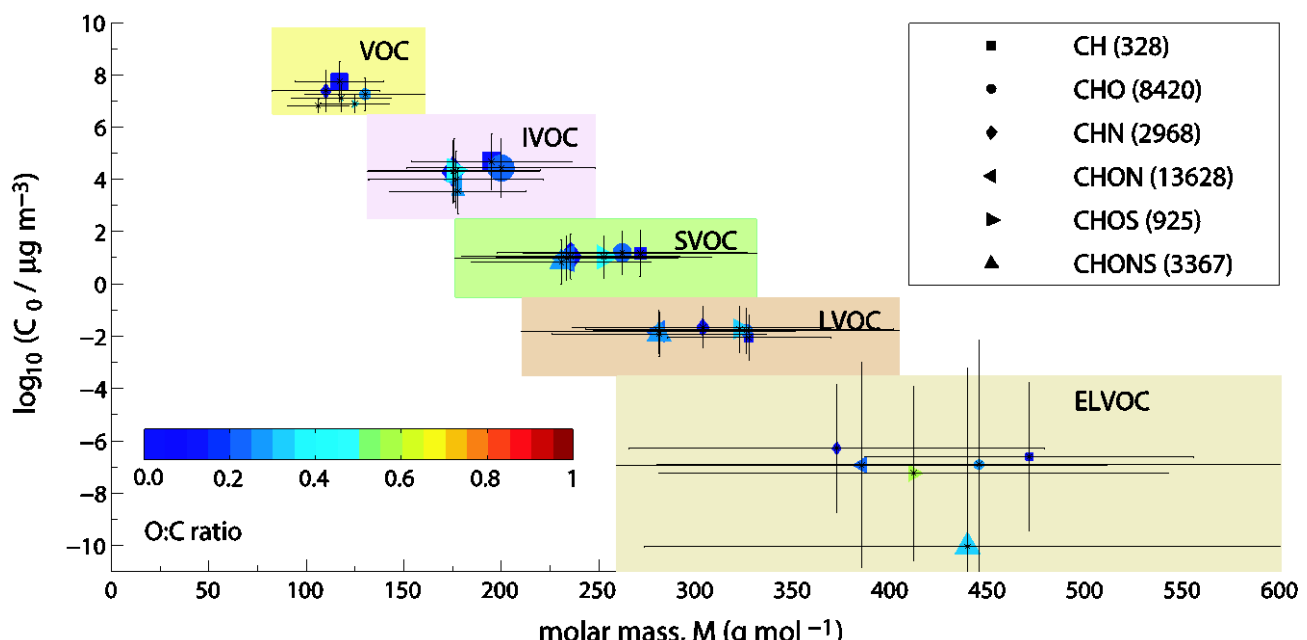
857 **Table 2.** Summary of the number of organic compounds in the composition classes (CH, CHO,
 858 CHN, CHON, CHOS, and CHONS) measured in 11 observation events.

Observations	CH	CHO	CHN	CHON	CHOS	CHONS	Total	References
<u>Experiments</u>								
New particle formation		55					55	Ehn et al., 2012 ^a ; Schobesberger et al., 2013 ^a
<u>Field</u>								
Forest	1	37	23	4	1		66	Ehn et al., 2010, 2012 ^a
Biomass burning			13	36		2	51	Laskin et al., 2009 ^b
Urban					212	37	249	Lin et al., 2012 ^b ; Stone et al., 2012 ^b ; Ma et al., 2014 ^b ; O'Brien et al., 2014 ^b ; Tao et al., 2014 ^b
Mt. Sonnblick	33	211	47	271	37	31	630	Holzinger et al., 2010 ^c
Fog		1425		711	218	83	2437	Mazzoleni et al., 2010 ^b
Cloud		1055		1985	357	544	3941	Zhao et al., 2013 ^b
Rain in New Jersey		192	6	320	129	52	699	Altieri et al., 2009a, 2009b ^b
Rain in Bermuda			50	734		27	811	Altieri et al., 2012 ^b
<u>Indoor</u>								
Reactions of skin lipids and O ₃	1	25					26	Wisthaler and Weschler, 2010 ^c
Tobacco smoke	20	42	13	13			88	Sleiman et al., 2010a, 2010b ^d

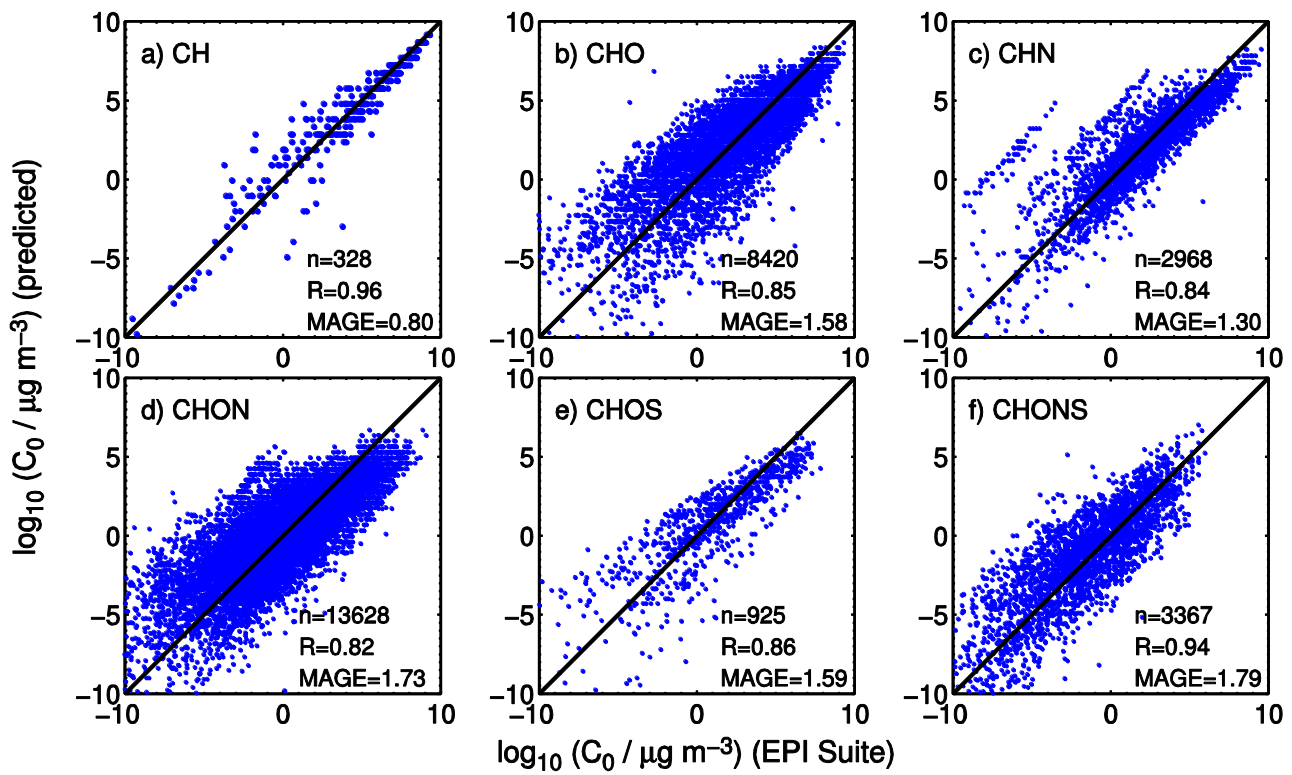
859 Applied analytical methods: ^a Atmospheric Pressure interface Time-Of-Flight mass spectrometry
 860 (APi-TOF-MS); ^b Electrospray ionization mass spectrometry(ESI-MS); ^c Proton-transfer-reaction
 861 mass-spectrometer (PTR-MS); ^d Gas chromatography mass spectrometry (GC-MS).



864 **Figure 1.** Molecular corridors of molar mass (M) vs. saturation mass concentration (C_0) for organic
865 compounds in elemental composition classes of **(a)** CH, **(b)** CHO, **(c)** CHN, **(d)** CHON, **(e)** CHOS,
866 and **(f)** CHONS. The data comprise 31,066 compounds from the NCI open database. The dotted
867 lines represent linear alkanes C_nH_{2n+2} (purple with O:C=0) and sugar alcohols $C_nH_{2n+2}O_n$ (red with
868 O:C=1). The small markers correspond to individual compounds identified in each structural
869 sub-class (see Sec. 2), color-coded by atomic O:C ratio. The larger symbols indicate the surrogate
870 compounds with the mean values of M , C_0 , and O:C ratio computed for each of the structural
871 sub-classes with error bars indicating standard deviations. Note that the data points above the linear
872 alkane line in Fig. 1(b) represent molecules with branched structures.
873



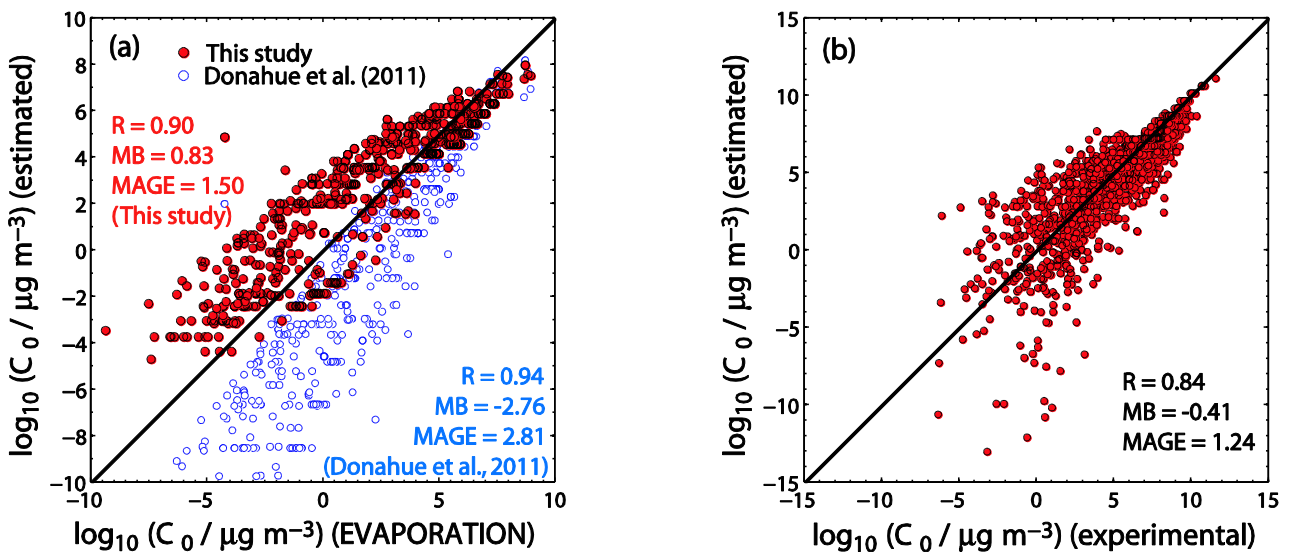
874
 875 **Figure 2.** Average molar mass (M), saturation mass concentration (C_0), and O:C ratio for organic
 876 compounds from the NCI database categorized by elemental composition (CH, CHO, CHN, CHON,
 877 CHOS, CHONS) and volatility (VOC, IVOC, SVOC, LVOC, ELVOC). The data points and error
 878 bars represent arithmetic mean values and standard deviations for each class of elemental
 879 composition. The symbol sizes are scaled by the number of compounds in each class. The center
 880 and borders of the colored boxes represent the mean and standard deviations of all compounds
 881 included in each volatility class.



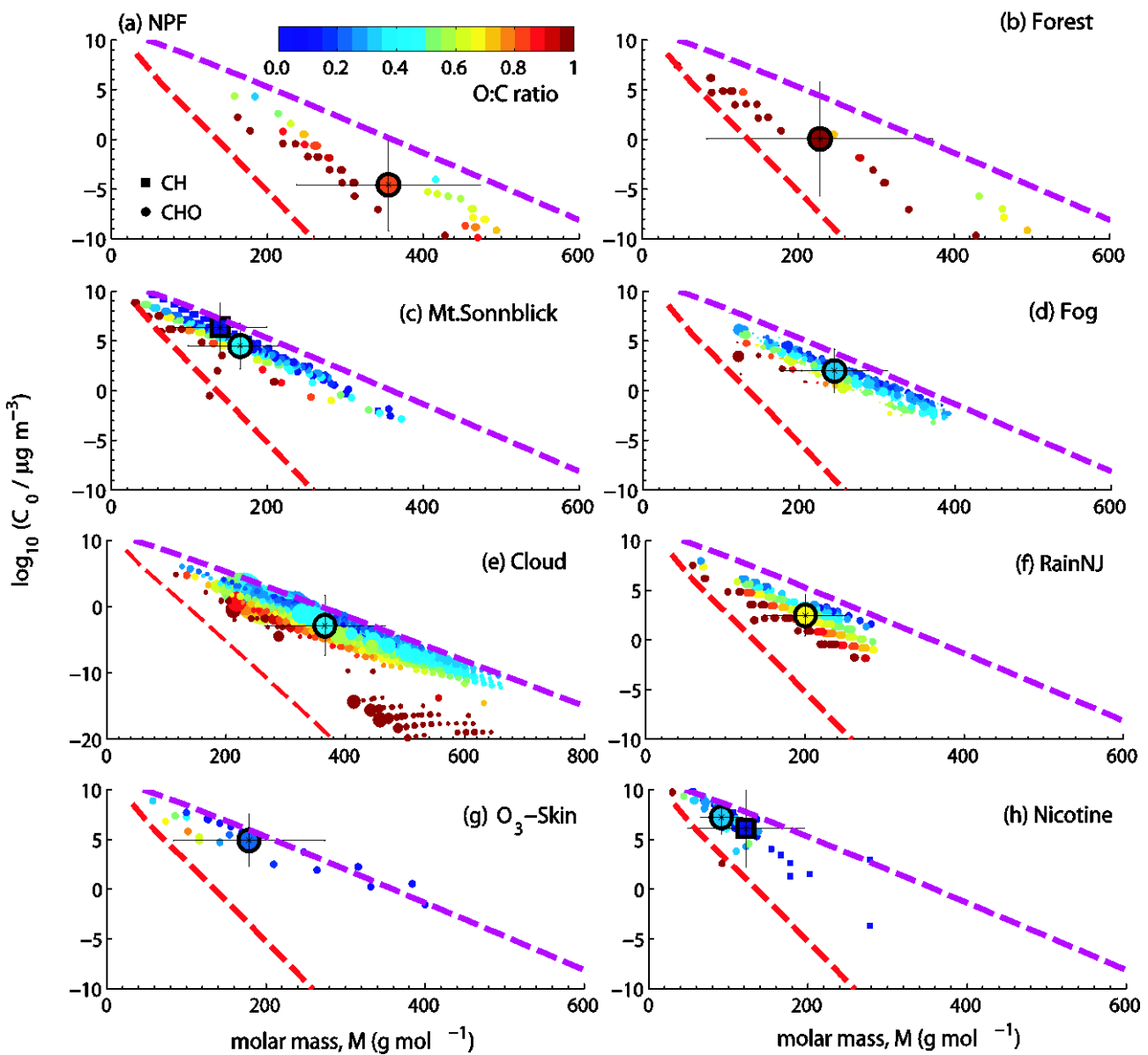
884
885

886 **Figure 3.** Saturation mass concentration (C_0) of organic compounds predicted by Eq. (2) from this
887 study plotted against C_0 determined by the EPI Suite software in the NCI database for elemental
888 composition classes of (a) CH, (b) CHO, (c) CHN, (d) CHON, (e) CHOS, and (f) CHONS.

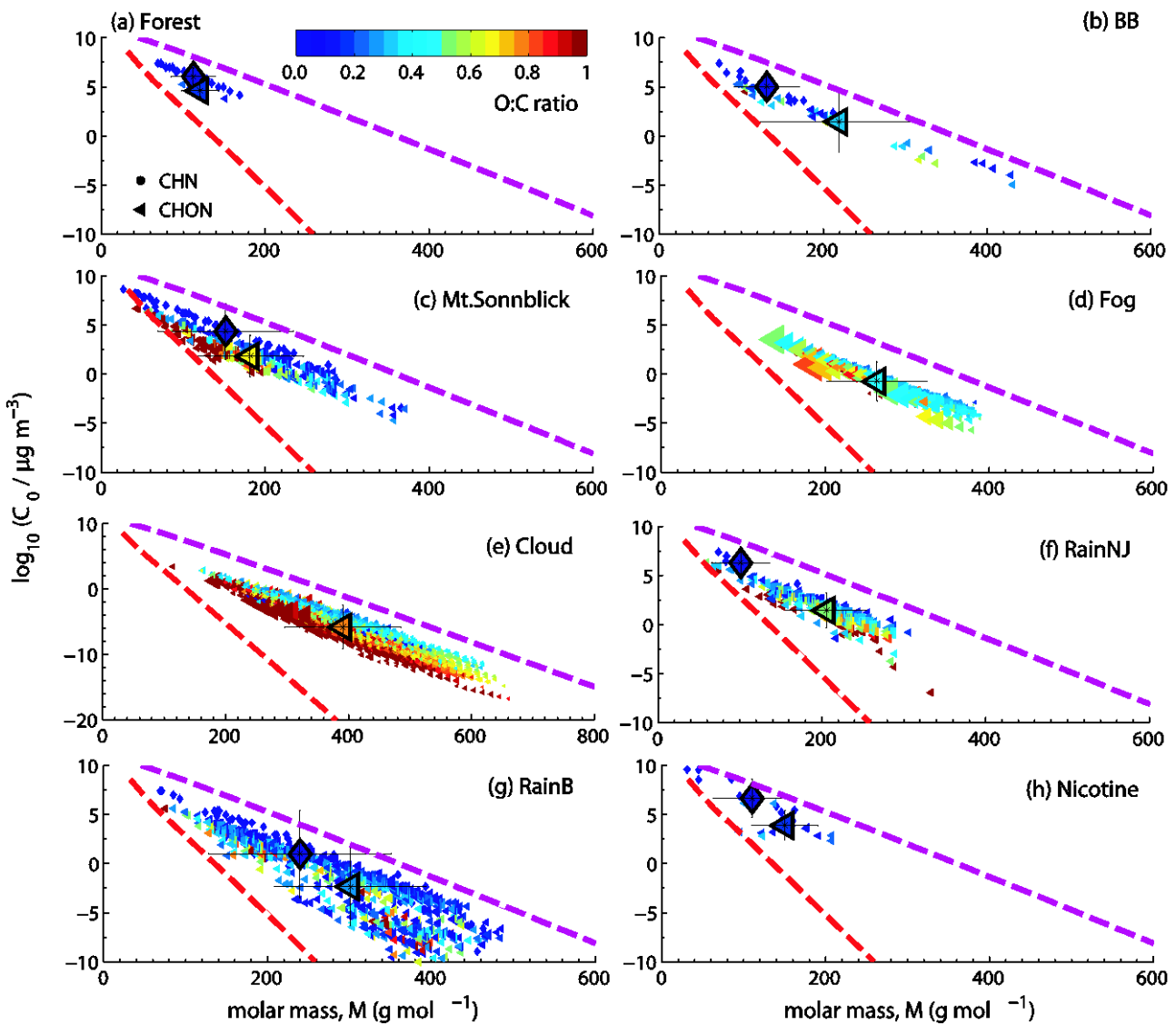
889
890
891
892
893
894
895
896
897
898
899
900



901
902 **Figure 4.** (a) Saturation mass concentration (C_0) of CHO compounds predicted by Eq. (2) with the
903 coefficients from this study and with the coefficients from Donahue et al. (2011) plotted against C_0
904 computed by the EVAPORATION model (Compernolle et al., 2011). The data comprise 704 SOA
905 oxidation products from biogenic (isoprene, α -pinene, limonene, glyoxal) and anthropogenic
906 precursors (C12 alkanes) as presented in Shiraiwa et al. (2014). (b) Comparison of C_0 predicted by
907 Eq. (2) in this study and experimental values taken from PHYSPROP Database
908 (<http://esc.syrres.com/interkow/EpiSuiteData.htm>).
909



911 **Figure 5.** Molecular corridors of saturation mass concentration (C_0) vs. molar mass (M) for CH and
912 CHO compounds measured in (a) chamber experiments for new particle formation (Ehn et al., 2012;
913 Schobesberger et al., 2013), (b) field campaigns conducted in the boreal forest of Hyttiala (Ehn et
914 al., 2010, 2012), (c) a field campaign conducted at Mt. Sonnblick (Holzinger et al., 2010), and
915 measurements of (d) fog in the city of Fresno (Mazzoleni et al., 2010), (e) clouds at Mt. Werner
916 (Zhao et al., 2013), (f) rain in New Jersey (Altieri et al., 2009a, 2009b), (g) indoor aerosols from
917 human skin lipids and ozone (Wisthaler and Weschler, 2010), and (h) tobacco smoke (Sleiman et al.,
918 2010a, 2010b). The small markers represent individual compounds identified in each data set
919 color-coded by atomic O:C ratio. The size of the small markers in (d) and (e) is linearly scaled by
920 relative intensity of MS signal. The larger symbols with error bars indicate surrogate compounds
921 with the mean values of M , C_0 , and O:C ratio computed for each data set.



922

923 **Figure 6.** Molecular corridors of saturation mass concentration (C_0) vs. molar mass (M) for
924 N-containing compounds collected from **(a)** boreal forest (Ehn et al., 2010, 2012), **(b)** biomass
925 burning (Laskin et al., 2009), **(c)** high alpine air at Mt. Sonnblick (Holzinger et al., 2010), **(d)** fog in
926 Fresno (Mazzoleni et al., 2010), **(e)** cloud at Mt. Werner (Zhao et al., 2013), **(f)** rain in New Jersey
927 (Altieri et al., 2009a, 2009b), **(g)** rain in Bermuda (Altieri et al., 2012), and **(h)** tobacco smoke
928 (Sleiman et al., 2010a, 2010b). The small markers represent individual compounds color-coded by
929 atomic O:C ratio. The size of the small markers in (d) and (e) is linearly scaled by relative intensity
930 of MS signal. The larger symbols with error bars indicate the surrogate compounds with the mean
931 values of M , C_0 , and O:C ratio (relative abundance considered for (d) and (e)).

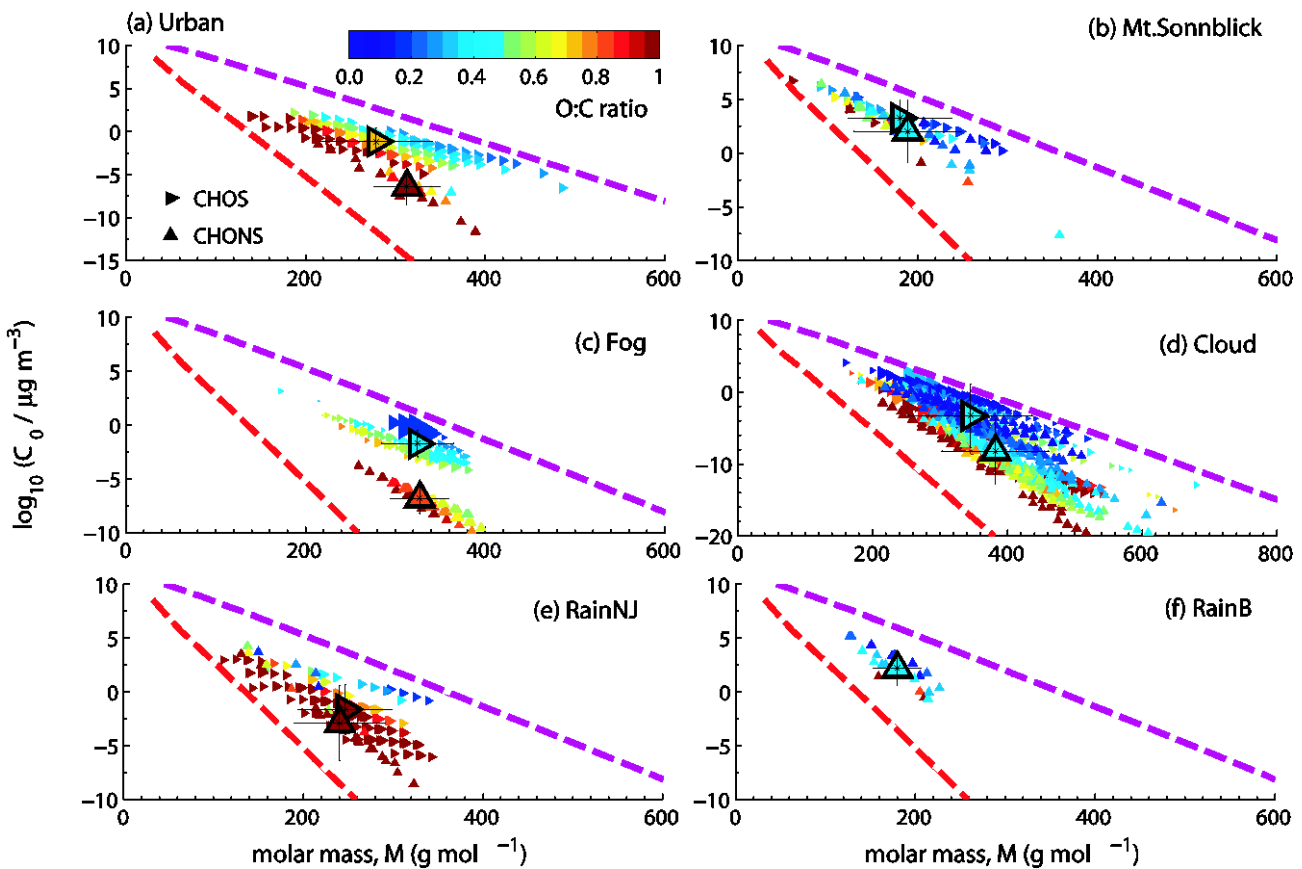


Figure 7. Molecular corridors of saturation mass concentration (C_0) vs. molar mass (M) for S-containing compounds collected from (a) urban areas including Shanghai (Ma et al., 2014; Tao et al., 2014) and Guangzhou (Lin et al., 2012), Taipei (Lin et al., 2012), Lahore (Stone et al., 2012), Bakersfield (O'Brien et al., 2014) and Los Angeles (Tao et al., 2014). (b) Mt. Sonnblick (Holzinger et al., 2010), (c) fog in Fresno (Mazzoleni et al., 2010), (d) cloud at Mt. Werner (Zhao et al., 2013), (e) rain in New Jersey (Altieri et al., 2009a, 2009b), and (f) rain in Bermuda (Altieri et al., 2012). The small markers represent individual compounds color-coded by atomic O:C ratio. The size of the small markers in (c) and (d) is linearly scaled by relative intensity of MS signal. The larger symbols with error bars indicate the surrogate compounds with the mean values of M , C_0 , and O:C ratio (relative abundance considered for (c) and (d)).

932

933

934

935

936

937

938

939

940

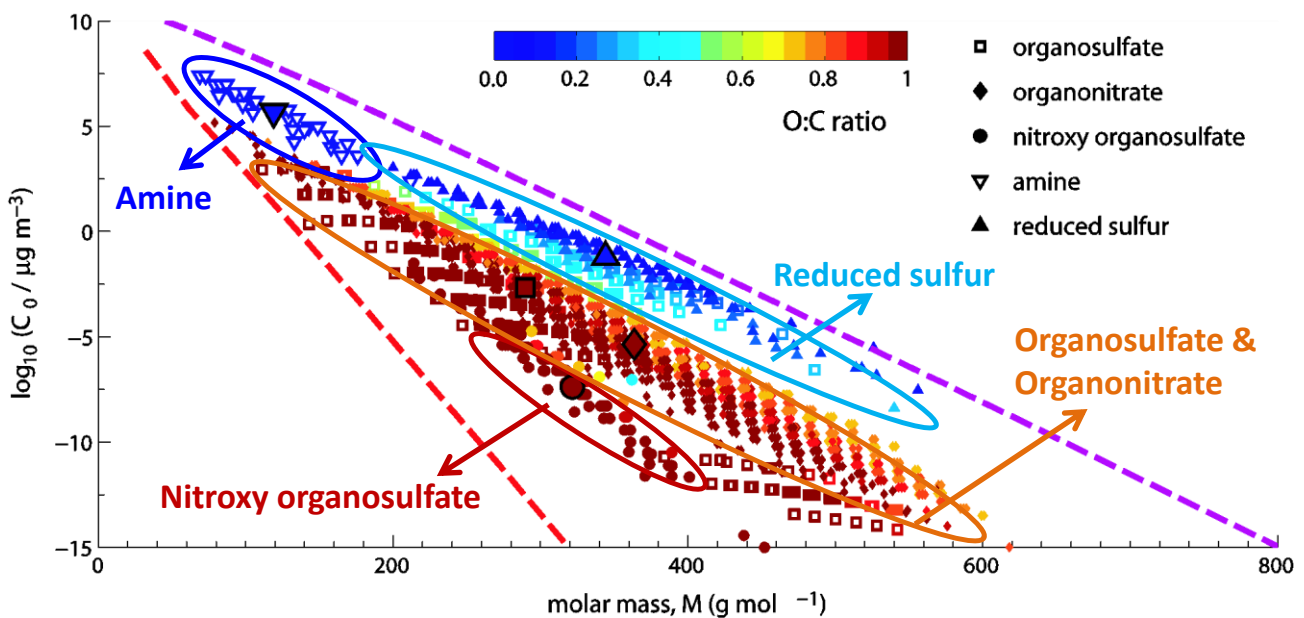
941

942

943

944

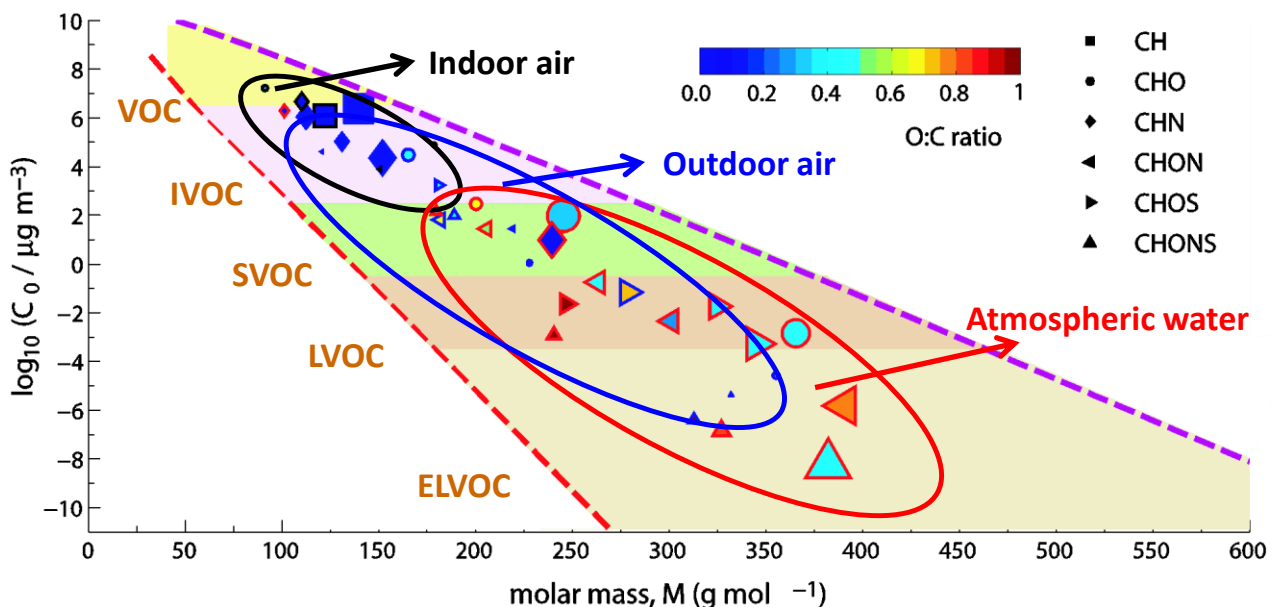
945



946

947 **Figure 8.** Molecular corridors of saturation mass concentration (C_0) vs. molar mass (M) for
948 organosulfate, organonitrate, nitroxy organosulfate, amine, and reduced sulfur compounds collected
949 from outdoor observations (Table 2). The small markers represent individual compounds
950 color-coded by O:C ratio. The larger symbols indicate surrogate compounds with the mean values
951 of M , C_0 , and O:C ratio.

952



953

954 **Figure 9.** Average molecular corridors for OA observed in indoor air, outdoor air, and atmospheric
 955 water. The markers show surrogate compounds with the mean values of molar mass (M), saturation
 956 mass concentration (C_0), and O:C ratio computed from every observation event (Figs. 5-7). The
 957 edge color of the symbols indicates the surrogate compound identified in indoor air (black), outdoor
 958 air (blue), and atmospheric water (red). The symbol size is scaled by the ratio of the number of
 959 compounds in each class (e.g., CH, CHO, CHON, CHONS) to the total number of compounds in
 960 each data set.

961